AD

RSIC-769

RECENT ADVANCES IN COHERENT OPTICS: FILTERING OF SPATIAL FREQUENCIES; HOLOGRAPHY

by

Serge Lowenthal
Yves Belvaux

Revue d'Optique, Theorique et Instrumentale,
46, No. 1, pp. 1-64 (1967)

Translated from the French

March 1968

REDSTONE SCIENTIFIC INFORMATION CENTER
REDSTONE ARSENAL, ALABAMA

JOINTLY SUPPORTED BY

U.S. ARMY MISSILE COMMAND

GEORGE C. MARSHALL SPACE FLIGHT CENTER

DISCLAIMER

The findings in this report are not to be constured as an official Department of the Army position unless so designated by other authorized documents.

DISPOSITION INSTRUCTIONS

Destroy this report when it is no longer needed. Do not return it to the originator.

28 March 1968 RSIC-769

RECENT ADVANCES IN COHERENT OPTICS: FILTERING OF SPATIAL FREQUENCIES; HOLOGRAPHY

by

Serge Lowenthal
Yves Belvaux

Revue d'Optique, Theorique et Instrumentale,
46, No. 1, pp. 1-64(1967)

Translated from the French

Translation Branch
Redstone Scientific Information Center
Research and Development Directorate
U. S. Army Missile Command
Redstone Arsenal, Alabama 35809

RECENT ADVANCES IN COHERENT OPTICS: FILTERING OF SPATIAL FREQUENCIES; HOLOGRAPHY

by

Serge Lowenthal
Yves Belvaux

Compagnie Generale de Telegraphic Sans Fil (CSF)
(General Wireless Telegraphy Company)

New applications of coherent light are presented:

a) Holography: recording of three-dimensional objects; diffuse illumination interferometry; reproduction of holograms; Fourier-transform holography and geometrical properties of holograms;

b) Spatial filtering: optical data processing, especially pattern recognition; automatic reading of characters, identification of fingerprints and other signals.

INTRODUCTION

Coherent optics is not a new field of physics: ever since Fresnel at the beginning of the 19th century there has been a succession of studies on luminous interference and diffraction phenomena.

However, the appearance in 1961 of the gas laser marks a discontinuity in this movement because of the rapid and considerable progress which has been accomplished since then in the field of coherent optics.

Two methods have particularly benefited from the increase in luminance, and in temporal and spatial coherence brought about by laser, compared with the classical sources:

a) The filtering of spatial frequencies in coherent light, thanks to the work of A. Marechal (1953) [1];

b) Holography, conceived by D. Gabor in 1948 [2] and subsequently perfected by the researchers of the University of Michigan [3,4].

In this paper we shall discuss the results of recent studies carried out under a DRME contract (Note: Contract 65-34-276 entitled "The Possibilities of Filtering of Spatial Frequencies") whose aim was to explore certain current possibilities of these methods.

In Chapter I we shall recapitulate certain elementary concepts relating to diffraction, in a form adapted to the problems treated subsequently.

Chapter II is devoted to the holograms. We know that the latter permit recording and then restitution on a photographic emulsion, with the aid of a coherent background, both the phase and the amplitude of a coherent light wave.

The results which we have obtained relate to the three-dimensional holograms (images in relief), to the duplication of holograms, to interferometry in diffuse light, to the formation of images by holography, and to Fourier-transform holography.

In Chapters III and IV we shall first recall the principles of the filtering of spatial frequencies, and will show that this method, based on diffraction in the optical instruments — a method which has yielded spectacular results in the improvement of optical images [5-7] — is in fact a method of data processing.

In effect, the coherent optical filtering implies a convolution relationship between two functions.

Convolution is a linear functional which comprises some important, special cases, notably the correlation, integration, differentiation, and scalar product of two functions.

It can be seen that by means of this mathematical apparatus it is possible to carry out data processing. It is this aspect of the problem which we have specially developed herein.

The fact that, on the one hand, this treatment is carried out in two dimensions (x,y) and that, on the other hand, it requires only a static filtering by a material screen whose transparency is suitably modulated, endows this method with great simplicity. Thus the optical correlation of two radar charts is as easy as that of two rectangular gating pulses.

In this way coherent optics makes its entry into an area which up to now has been reserved for electronic computers.

In Chapter IV the optical filtering is applied to pattern recognition. This term actually comprises some highly diverse processes, all of which,

however, are treated by an analogous formalism. A satellite detection system, for example, gives a signal from which a number of data are expected such as presence, position or velocity; this is a form of pattern recognition.

Among the results presented herein, we have stressed the automatic recognition of characters in a printed text. In effect, despite its apparent simplicity, this problem is beset with a number of traps whose solution makes it possible to approach other problems, such as the treatment of electric signals after spatial transposition, with a greater hope of success.

The study presented herein makes no claims for being exhaustive; the subject is in the process of development, as is shown by the bibliographical references given at the end of this article.

I. GENERAL DISCUSSION OF DIFFRACTION

1. Introduction

Coherent optics is based on the phenomena of diffraction. Below we shall discuss some of the elements of the theory of diffraction used in this study, particularly the form of the correspondence between two planes, one of them comprising an illuminated aperture which diffracts the light, and the other being the observation plane.

In the mathematical expressions for this correspondence there appear certain pure phase factors which are frequently neglected, because they disappear during recording done by means of detectors such as the photographic plate.

In holography and in the filtering of spatial frequencies these terms play an important role: it is for this reason that an effort is made to show them in the formulas which will be developed in the case of

a) Fraunhofer's diffraction, relating to observation in the vicinity of a focus, or at infinity;

b) Fresnel's diffraction, relating to all other cases.

These two cases are deduced from the analytical expression of Huygens' principle.

2. The Huygens-Fresnel Transformation Principle

This principle may be stated as follows:

If the electromagnetic field (produced by a coherent source) is known on a closed surface S which does not contain any sources in its interior (Figure 1), it is known at any point P in the interior of surface S.

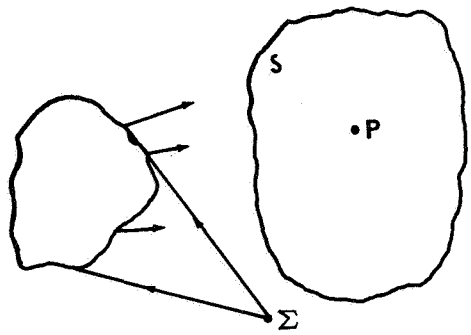

Figure 1. Huygens' Principle. If the electromagnetic field is known on a closed surface S not containing any sources such as Σ, it is known at any point P located within S.

It is in this form that Huygens' principle will be used in the overall study of the holograms.

The analytical expression of the phenomena is easy only when the surface is an absorbing plane Π_o pierced by an aperture. Plane Π_o is completed by the half-sphere of infinity whose contribution at P is zero.

For an optical instrument the diffracting opening is the exit diaphragm.

Let Π_o be the diffracting plane (Figure 2). We shall now determine the complex amplitude of the electromagnetic field diffracted by Π_o at point P situated in a plane $\mathcal{F}$ parallel to Π_o.

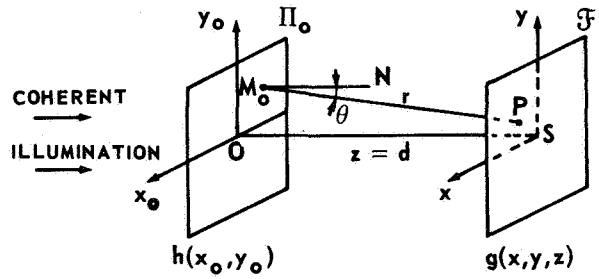

Figure 2. Fresnel's Diffraction. Π_o is the diffracting plane; $\mathcal{F}$ is the observation plane.

This result can be obtained by means of several expressions. We shall use Sommerfeld's formula [8]:

$$(I.1)\quad g(x,y,z) = \frac{e^{-i\omega t}}{2\pi}\int\int_{\Pi_o} h\left(x_o,y_o\right)e^{ikr}\cos\theta\left(\frac{ik}{r} - \frac{1}{r^2}\right)dx_o\,dy_o \ ,$$

where $h\left(x_o,y_o\right)$ is the complex amplitude at a point M_o having coordinates x_o,y_o in plane Π_o of origin O; $g(x,y,z)$ is the diffracted amplitude at point $P(x,y,z)$, r is the distance M_oP, θ is the angle between M_oP and the normal, M_oN to Π_o, and $k = 2\pi/\lambda$, the wave number.

Formula (I.1), valid in the scalar approximation for a quasi-monochromatic wave of pulsation ω, is simplified when the diffraction angles are small. We then have $\cos\theta \simeq 1$. If, moreover, the distance $z = d$ between $\mathcal{F}$ and Π_o is large compared with λ, we can neglect $1/r^2$ compared with ik/r, and take this last term outside the integral, because $r \simeq z = d$, whence, we have

$$(I.2)\qquad g(x,y,d) = -\frac{i}{\lambda d}\int\int_{\Pi_o} h\left(x_o,y_o\right)e^{ikr}\,dx_o\,dy_o \ .$$

In factor e^{ikr}, we have

$$(I.3)\qquad r = \left[d^2 + \left(x - x_o\right)^2 + \left(y - y_o\right)^2\right]^{1/2} \ ;$$

Now, d is large compared with the other terms, and (I.3) may be expanded:

$$(I.4)\qquad r \simeq d + \frac{1}{2d}\left[\left(x - x_o\right)^2 + \left(y - y_o\right)^2\right]$$

and expression (I.2) becomes

$$(I.5)\qquad g(x,y,d) = -\frac{i}{\lambda d}e^{ikd}\int\int_{\Pi_o} h\left(x_o,y_o\right) \times \exp\left\{\frac{ik}{2d}\left[\left(x - x_o\right)^2 + \left(y - y_o\right)^2\right]\right\}dx_o\,dy_o \ .$$

This expression will serve as the point of departure for establishing the properties of both Fresnel's and Fraunhofer's diffraction.

Vectorial Notation. Vector $\vec{OM}_o$ of components x_o, y_o, contained in plane Π_o, will be denoted as M_o. Likewise vector $\vec{SP}$ of components x, y, contained in plane $\mathcal{F}$ will be denoted as P.

We shall also write

$$h(x_o, y_o) = h(M_o), \qquad g(x,y,d) = g(P,d),$$
$$dx_o\, dy_o = dM_o, \qquad dx\,dy = dP.$$

With these conventions, the term $(x - x_o)^2 + (y - y_o)^2$ becomes the scalar square $(P - M_o)^2$ and when expanded becomes $P^2 + M_o^2 - 2PM_o$, the term PM_o being the scalar product of P and M_o.

The analytical form (I.5) of the Huygens-Fresnel principle is therefore written as

$$(I.6) \qquad g(P,d) = -\frac{i}{\lambda d} e^{ikd} \int_{\Pi_o} h(M_o) \exp\left[\frac{ik}{2d}(P - M_o)^2\right] dM_o \ .$$

3. Fresnel Diffraction and Fresnel Transformation

Expression (I.6) gives the complex amplitude of the field diffracted by plane Π_o at a point P situated at a finite distance from Π_o; hence this is a Fresnel phenomenon.

When the observation is made in a plane $\mathcal{F}$ parallel to Π_o, the factor in front of the integral is a constant which may be neglected; hence, by writing $g(P)$ for $g(P,d)$, (I.6) becomes

$$(I.7) \qquad g(P) = \int_{\Pi_o} h(M_o) \exp\left[\frac{ik}{2d}(P - M_o)^2\right] dM_o \ ,$$

which can be further written as

$$(I.8) \qquad g(P) = e^{ikP^2/2d} \int_{\Pi_o} h(M_o) \exp\left[\frac{ik}{2d}(M_o^2 - 2P.M_o)\right] dM_o \ .$$

If phenomenon (I. 8) is recorded by photographic plate which is sensitive only to illumination $|g(P)|^2$, the quadratic factor exp $(ikP^2/2d)$ disappears and may be neglected in the formulas. By contrast, in holography this factor is recorded, and hence the complete expression (I. 7) must be preserved.

Relation (I. 7) is a convolution product symbolically denoted as

$$g(P) = h(P) \ast e^{ikP^2/2d} \quad . \tag{I.9}$$

This expression is a Fresnel transformation. It can be shown that the latter is reciprocal, i.e., if we have (I. 9) we also have

$$h\left(M_o\right) = \frac{1}{\lambda^2 d^2}\, g\left(M_o\right) \ast e^{-ikM_o^{\,2}/2d} \quad . \tag{I.10}$$

The two relations (I. 9) and (I. 10) express, for the Fresnel diffraction, the correspondence between a diffracting plane Π_o and an observation plane $\mathcal{F}$; the roles of the two planes may be reversed.

Special Case. The diffracting plane Π_o is reduced to a luminous point M, and then $h\left(M_o\right)$ is represented by the Dirac distribution $\delta\left(M - M_o\right)$ and the distribution of the complex luminous amplitudes on $\mathcal{F}$ becomes

$$g(P) = \exp\left[\frac{ik}{2d}(M - P)^2\right] \quad , \tag{I.11}$$

a result which is readily obtained also by a direct calculation.

4. Fraunhofer's Diffraction and Fourier Transformation

Fraunhofer's diffraction takes place in the vicinity of the focus S (in the general sense) of an optical system (Figure 3), the latter being characterized by its exit diaphragm Π_o (real or virtual). Point S is the paraxial image of a point — and monochromatic source S_o.

Let $\mathcal{F}$ be the plane parallel to Π_o, with origin S and with position vector P.

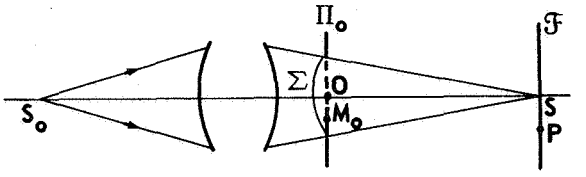

Figure 3. Fraunhofer's Diffraction. The diffracting plane Π_o is the exit pupil of an optical instrument. The observation plane $\mathcal{F}$ is normal to the axis at S, which is the paraxial image of a monochromatic point source S_o.

To study the amplitude g(P) diffracted on the plane $\mathcal{F}$ by pupil Π_o, we use form (I.6) of Huygens' principle which, as we have just seen, relates to the Fresnel diffraction at a finite distance. However, the intervention of the optical system modifies this expression.

In effect it is necessary to introduce in (I.6) the distribution of amplitudes $h(M_o)$ on plane Π_o; the distribution is given by the amplitude which would be produced on Π_o by the perfect spherical wave Σ which converges in S, in the absence of diffraction (since the diffraction intervenes only after passage through screen Π_o); whence, if r_o is the radius of Σ,

$$h(M_o) = e^{-ikr_o} . \tag{I.12}$$

By means of a reasoning similar to that of Paragraph I.2 we obtain, in vectorial notation,

$$r_o = M_oS = d + \left(M_o^2/2d\right) . \tag{I.13}$$

Hence, after taking the independent term of M_o outside the integral and taking (I.12) and (I.13) into account, formula (I.6) becomes, save for the constant factor $-i/\lambda d$,

$$g(P) = e^{ikP^2/2d} \int_{\Pi_o} \exp\left(-\frac{ik}{d} P.M_o\right) dM_o . \tag{I.14}$$

In this calculation we have assumed that the transparency of pupil Π_o is uniform. If this transparency is not uniform but represented by the complex function $f(M_o)$, (I.12) becomes

$$h(M_o) = f(M_0)e^{-ikr_o} . \tag{I.15}$$

This situation occurs especially in the filtration of spatial frequencies where a photographic plate of transparency $t = f(M_o)$ is placed against Π_o.

Under these conditions we obtain, instead of (I.14),

$$g(P) = e^{ikP^2/2d} \int_{\Pi_o} f(M_o) \exp\left(-\frac{ik}{d} P.M_o\right) dM_o \tag{I.16}$$

which, save for the factor

$$e^{ikP^2/2d} \tag{I.17}$$

is the Fourier transform of $f(M_o)$.

To obtain (I.16) we have started out from formulas relating to the Fresnel phenomena, but the introduction of the term (I.12), due to the sphericity of wave Σ, gives a Fourier's transform as a final result save for factor (I.17).

a. The Quadratic Phase Factor

As the case of the Fresnel diffraction (Paragraph I.3) the factor (I.17) is frequently neglected — because it disappears during the recording of the phenomenon (I.16) by means of a cell or a photographic emulsion. In coherent optics it is no longer permitted to ignore it; in effect:

1) In Fourier-transform holography (I.17) is recorded, and it changes the properties of the hologram. We shall return to this point in Chapter IV;

2) In the filtering of spatial frequencies it is necessary to compensate (I.17) in order to obtain linear relations invariant by translation.

b. Reciprocity of the Fourier Transformation

The presence of the quadratic phase factor (I.17) (which represents a spherical wave) means that the Fourier transform of function $f(M_o)$ is not formed on plane $\mathcal{F}$ but on a sphere of radius d, with its center in O.

Factor (I.17) will often be compensated below (Chapter III); the distribution (I.16) of the amplitudes on plane $\mathcal{F}$ then becomes the Fourier integral

(I.18) $$F(P) = \int_{\Pi_o} f\left(M_o\right)\exp\left(-\frac{ik}{d}\, P.M_o\right)dM_o \quad .$$

We know that this transformation is reciprocal and that we have

(I.19) $$f\left(M_o\right) = \frac{1}{\lambda^2 d^2}\int_{\mathcal{F}} F(P)\exp\left(\frac{ik}{d}\, P.M_o\right)dP \quad .$$

c. Reduced Coordinates

Let us write (Figure 4) for coordinates x and y of point P of the Fourier plane $\mathcal{F}$.

(I.20) $$u = x/\lambda d, \qquad v = y/\lambda d;$$

where u and v are the reduced coordinates of P which define the vector $\Omega(u,v)$ of the Fourier space.

Hence relations (I.18) and (I.19) become, save for a constant factor,

(I.21) $$F(\Omega) = \int_{\Pi_o} f\left(M_o\right)\exp\left(-2\pi i\Omega.M_o\right)dM_o \quad ,$$

(I.22) $$f\left(M_o\right) = \int_{\mathcal{F}} F(\Omega)\exp\left(2\pi i\Omega.M_o\right)d\Omega \quad ,$$

which corresponds to the usual notation of the Fourier transformation.

d. Notations for the Fourier Transformation

We shall generally use for a pair of Fourier transforms the same pair of letters, one of them being a lower case letter and the other one a capital letter.

We shall also write, for the Fourier transformation (I.21),

(I.23) $$f\left(M_o\right) \xrightarrow{F.T.} F(\Omega)$$

(F.T. = Fourier transformation)

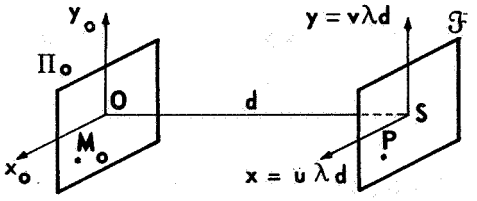

Figure 4. The Reduced Coordinates. If x and y are the coordinates in the Fourier plane, the reduced coordinates $u = x/\lambda d$, $v = y/\lambda d$ define the vector $\Omega(u,v)$ of the Fourier space.

and for the inverse Fourier transformation

$$F(\Omega) \xrightarrow{F.T.^{-1}} f(M_o) \quad . \tag{I.24}$$

Notes.

a) The time factor chosen is $e^{-i\omega t}$; hence the phase lags are positive.

b) In line with the usage adopted in optics we shall frequently use the term "amplitude" for "complex amplitude."

5. Conclusion

A large number of diffraction problems may be solved by the approximate formulas (I.9) and (I.16) relating to the Fresnel and Fraunhofer diffractions.

When the diffraction angles are large, formula (I.2) gives satisfactory results within the limits of the scalar approximation (study of the aberrations of the holograms).

Finally it should be remembered — and this is often useful in certain reasonings (for example, Paragraph II.7) — that Huygens' principle may be strictly expressed, with the aid of a Green function, by a convolution.

II. HOLOGRAMS

1. Introduction

Holography has introduced considerable progress into coherent optics. While originally the purpose of the holograms was to reconstitute two- or three-dimensional images from a photographic recording made without lenses, their present field of application is much more widespread.

Hence the term "lens-less photography" gives a rather restrictive meaning to this method, and it is more accurate to use the expression "recording of a coherent optical wave in phase and in amplitude."

In effect it is here that the interest of holography resides. By means of a coherent background it is possible to record any diffraction phenomenon on a photosensitive material. This phenomenon may then be restituted at will by coherent illumination of the photographic emulsion. In particular, if the diffracted wave originates from a three-dimensional object, the image of this object in relief is reconstituted, but in the case of a randomly chosen wave its manipulation is the equivalent of that of a photographic plate.

Another remarkable property of holograms is that it is possible to record, successively, several waves on the same emulsion. In that case the process taking place during the restitution is an addition not of the intensity but of amplitude and phase.

The principle of holograms is now sufficiently well known to enable us to take up its study in the form of a general method which is frequently fruitful in research.

We shall stress more specifically the new aspects obtained herein:

a) Properties of holographic image production by a simple geometric method;

b) Diffuse illumination interferometry;

c) Duplication of holograms;

d) Applications to the filtering of spatial frequencies (Chapter IV);

e) Experimental results in three-dimensional holography.

2. Physical Aspect of Holography

The idea which led to holography [2-4] was based on the Huygens-Fresnel principle and on the properties of luminous interferences.

Let us take at random a diffracting system which emits a coherent electromagnetic wave. This system is represented schematically in Figure 5 by an object O illuminated by a laser $\mathcal{L}$.

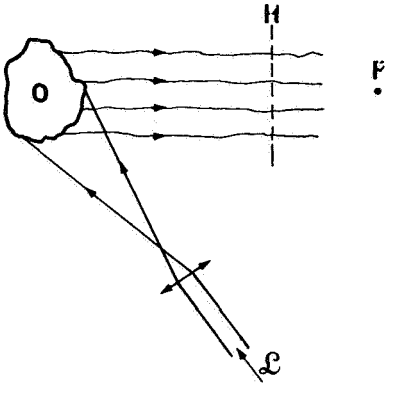

Figure 5. Huygens' Principle. The radiation received by point P may be considered as originating either from object O illuminated by laser ℒ, or from a random virtual plane H situated between O and P.

Let us take, in addition, a point P which receives the radiation emitted by O, and a virtual plane H situated between O and P. The wave emitted by object O passes through plane H before arriving at P. Thus it can be said that the radiation received by P originates from the object, that it can likewise be said that it originates from the virtual plane H.

Let us now consider the following two situations:

a) The object illuminates point P and gives a distribution of complex amplitudes $A(x,y,t)$ on plane $H(x,y)$;

b) The object is absent, but a synthetic source has been reconstituted on H; the vibrational state of this source is $A(x,y,t)$.

According to the Huygens-Fresnel principle the effect at P is the same for both situations.

A hologram is precisely a photographic recording which, when illuminated in a suitable manner, restitutes the wave $A(x,y,t)$.

However, we know that it is not sufficient to place a photographic emulsion in plane H in order to obtain such a recording. In effect the progressive monochromatic wave emitted by O will give, on plane H, the field distribution

$$A(x,y)\cos[\omega t - \varphi(x,y)] \quad , \tag{II.1}$$

but the blackening produced on the plate will be a function only of the received energy, proportional to the mean, in time, of the square of (II.1), i.e., to

$$[A(x,y)]^2 \tag{II.2}$$

and the phase information will be lost.

To preserve both the phase and the amplitude information (II.1) is transformed into a stationary wave by the addition of a coherent background. In this way we obtain a network of interference fringes whose recording constitutes the hologram. The local variation of the contrast of the fringes and of the fringe interval in the interferogram then reflects the local variation of the amplitude and the phase of the wave (II.1).

Experimental Arrangement. The coherent background is added simply by means of the assembly whose schematic outline is shown in Figure 6.

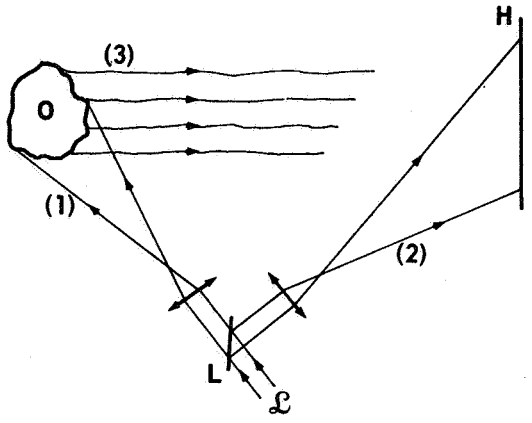

Figure 6. Recording of a Hologram: Principle of the Assembly. A laser beam £ is separated into two waves (1) and (2), by the separating L. Wave (1) illuminates object O. The reference wave (2) directly illuminates the photographic emulsion H; it constitutes the coherent background which interferes with wave (3) diffracted by the object. The plate records the total illumination due to waves (2) and (3).

The coherent background is also called carrier or reference wave.

Let us examine this process in greater detail, as well as the manner in which hologram H restitutes the recorded wave.

3. Principle of the Holograms

The experimental arrangement of Figure 6 is reproduced in a schematic manner in Figure 7. The same laser — not represented — illuminates the object and gives the reference wave. The object may be illuminated in any manner; for example one may interpose a polished glass between the laser and the object.

The reference wave is generally a parallel, divergent or convergent, wave; hence it may be represented by a point source S_p.

a. Recording of the Holograms

We use the subscript o for the object and p for the carrier. The coordinates on H are x and y.

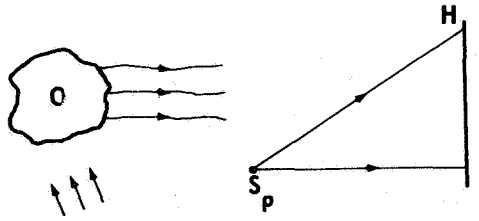

Figure 7. Recording of the Hologram (Shown Schematically). A laser illuminates the object in any given manner (if necessary through a polished glass). A part of the laser beam serves for forming the point reference source S_p. The hologram is recorded on H.

The object diffracts on H — neglecting the time factor $e^{-i\omega t}$ — the complex amplitude

$$A_o(x,y) = a_o(x,y)\exp\left[i\varphi_o(x,y)\right] \quad . \tag{II.3}$$

This distribution is unknown a priori, but is perfectly well defined because the illumination is coherent.

The carrier gives, on H, the complex amplitude

$$A_p(x,y) = a_p(x,y)\exp\left[i\varphi_p(x,y)\right] \quad . \tag{II.4}$$

Plate H records the total illumination due to (II.3) and (II.4), or

$$I = \left|A_o + A_p\right|^2 = \left|A_p\right|^2 + \left|A_o\right|^2 + A_o A_p^* + A_o^* A_p \quad . \tag{II.5}$$

The amplitude transparency t of the plate on which the image is produced is proportional, if γ is the slope of the characteristic curve of the emulsion, to (Appendix 2)

$$t = I^{-\gamma/2} \quad . \tag{II.6}$$

To free ourselves from the influence of the properties of the emulsion and to make the recording linear we bring about the following relationship (which can be easily done experimentally)

$$\left|A_p\right| \gg \left|A_o\right| \quad . \tag{II.7}$$

Then we can undertake an expansion of (II.6); we obtain, keeping (II.5) in mind,

$$(II.8) \qquad t = |A_p|^{-\gamma}\left(1 - \frac{\gamma}{2}\left|\frac{A_o}{A_p}\right|^2 - \frac{\gamma}{2}\frac{A_o A_p^*}{|A_p|^2} - \frac{\gamma}{2}\frac{A_o^* A_p}{|A_p|^2} + \ldots\right) .$$

The reference wave is generally plane or spherical; hence, with the approximations usually made in diffraction, it produces an illumination $|A_p|^2$ which is constant on H and which will be standardized as 1:

$$(II.9) \qquad |A_p|^2 = a_p^2 = 1 .$$

Condition (II.7) makes it possible to neglect the term $(\gamma/2)\left|A_o/A_p\right|^2$. Hence (II.8) may be written, except for the constant $|A_p|^{-\gamma}$ which represents a uniform absorption of the holograms,

$$(II.10) \qquad t = 1 - \frac{\gamma}{2} A_o A_p^* - \frac{\gamma}{2} A_o^* A_p .$$

In this way we obtain an expression which does indeed contain the amplitude and the phase of the diffracted wave, because (II.10) can also be written as

$$t = 1 - \gamma a_o(x,y)\cos\left[\varphi_o(x,y) - \varphi_p\right] .$$

In this form the interferential aspect can be readily seen. It may be noted that (II.10) is real and positive, and the complex recorded wave (II.3) appears only by diffraction during the restitution.

b. Reconstruction

Hologram (II.10) is illuminated by a reconstruction wave A_r which is identical to the reference wave (II.4) which was used during the recording; this is not indispensable, as we shall see later, but the demonstration of this process is simplified. Thus on the minus face of the hologram (Figure 8) the amplitude is

$$(II.11) \qquad A_r = A_p .$$

On the plus face of H the transmitted amplitude is $A_i = tA_r$, or

$$(II.12) \qquad A_i = A_r - \frac{\gamma}{2} A_o A_p^* A_r - \frac{\gamma}{2} A_o^* A_p A_r$$

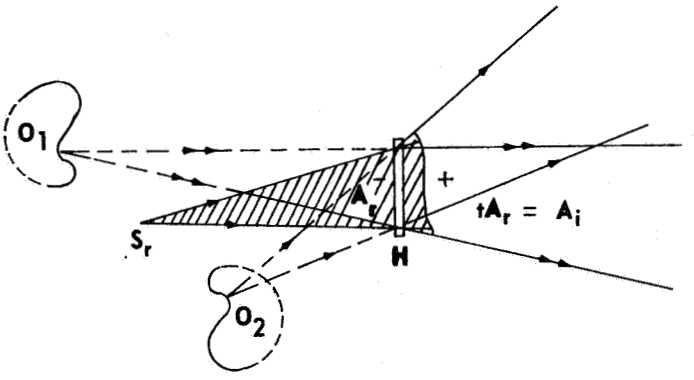

Figure 8. Reconstruction of the Hologram. The reconstruction source S_r illuminates the hologram H. The latter transmits three waves: 1) the slightly altered reconstructed wave (cross-hatched); 2) two waves originating from two reconstructed images O_1 and O_2. The two images may be real or virtual, or partly virtual and partly real, depending on the position of S_r at reconstruction. If S_r is identical with the reference source S_p (Figure 7), one of the images is identical to the recorded object and is situated in the same region.

This is the general expression of the amplitude transmitted by the hologram. Keeping in mind (II. 9) and (II. 11), it becomes

$$A_i = A_r - \frac{\gamma}{2} A_o - \frac{\gamma}{2} A_r^2 A_o^* \quad . \tag{II. 13}$$

Thus the hologram reconstructs three waves.

1) The first term A_r of (II. 13) corresponds to the directly transmitted reconstructed wave. In reality this wave is slightly perturbed by the term $-(\gamma/2)\left|A_o/A_p\right|^2$ which was neglected when going from (II. 8) to (II. 10).

2) The second term represents, save for the factor $-\gamma/2$, the amplitude A_o diffracted by object O on H during the recording; hence this wave is

wholly reconstituted in phase and in amplitude. An observer situated to the right of H will, in particular, see a three-dimensional image O_1 having all the characteristics of object O: relief, parallax and depth of field (Figures 17 through 26). If object O is a wave surface given by any given coherent system, this wave surface will have been reconstituted.

3) The third term, $-(\gamma/2)\, A_r^2 A_o^*$, represents a second reconstituted image O_2 which will be called conjugated image, as distinct from image O_1 which is called direct image. The properties of the conjugate image will be completely defined in the study of a point object and source presented in Paragraph II. 5. Let us note, for the time being, that this image may be virtual, real or partly virtual and partly real, depending on the operating conditions.

4. Notes on the Holograms

Several conclusions may be drawn from the reasonings just made.

a) The γ of the emulsion (expression II. 13) intervenes only in the form of a constant factor in the amplitude of the waves diffracted by the hologram. The sign of γ, which is + for a negative emulsion and - for an inversible emulsion, fixes the phase of the diffracted waves to within π. Hence a copy of a hologram, which reverses the sign of γ, has the same properties as the original hologram. This fact, in particular, makes it possible to use the method of hologram reproduction proposed in Paragraph II. 8.

b) Contrary to general photography which consists of a point-by-point correspondence, a hologram results from the point-(whole) object plane correspondence of the hologram. Hence it has been proposed that any given portion of the hologram is sufficient to reconstruct the whole object. While this is true for diffusing objects which are then rendered with a decreased resolution and at a given angle, this is no longer true for nondiffusing objects. In particular, in Fourier holography (Filtering of the Spatial Frequencies, Chapter IV) a given portion of the hologram permits the reconstruction of only some spatial frequencies of the object. For a periodic object it is even possible that nothing is reconstructed from the whole.

In interferential holography a portion of the hologram permits the obtainment of only a portion of the interferogram of the same order of magnitude. This has led us to develop an interferential method in diffuse light.

c) The angular separation between the three transmitted beams is due to the use of an "inclined" carrier. In first approximation this means simply that the cone, defined by the carrier resting on the contour of the hologram, need not contain the object. Thus a separation can take place even when the carrier

is not inclined but is normal to the plate. The geometric study contained in Paragraph II. 5 makes it possible to treat these field problems in an easy manner.

5. Geometric Study of the Holograms

Now that we are familiar with the principle of holography, we can make a purely geometric study of the formation of the images by the holograms. The latter, in effect, have numerous analogies with lenses.

The formulas proposed below seem to be easier to use than those given elsewhere in the literature [9,10]. In effect the axes of the different beams involved in the holographic technique are different ones; thus one has the advantage of using polar coordinates which simplify the results and their interpretation.

We shall conduct our reasoning, as in classical geometric optics, on a point object M_o which in this case gives two images M_1 and M_2. The reference wave (carrier) is emitted from a point source S_p and the restitution wave from a point S_r. Points M_o, S_p, and S_r have arbitrary positions; they may be real or virtual, at a finite distance or at infinity.

We shall examine successively the formation of the images in the meridian plane and outside the meridian plane.

a. Formulas in the Meridian Plane

(1) Notations (Figure 9). Points M_o, S_p, and S_r are defined by their "polar" coordinates $(\rho,\theta)_{o,p,r}$. The radius vectors ρ have their origin in any given point C of hologram H. The latter is situated in plane $z = 0$.

(2) Sign Conventions. The ρ's are negative for $z < 0$ and positive for $z > 0$. The θ's are marked off as on the figure, in space $z > 0$. They are positive in the counterclockwise direction. The origin of the angles is axis Cz. $|\theta|$ is always $<\pi/2$.

(3) Establishment of the Conjugation Formulas. On recording, points M_o and S_p diffract amplitudes A_o and A_p on H. On restitution the source S_r diffracts amplitude A_r on H.

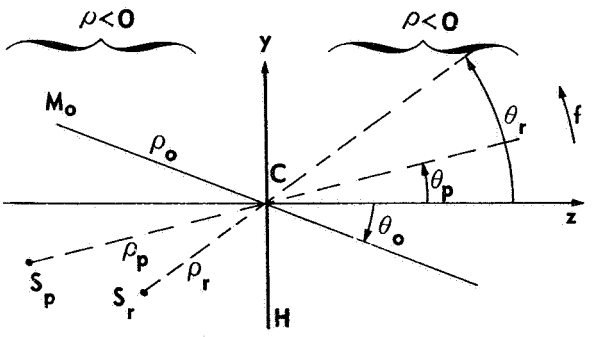

Figure 9. Geometric Study of Holograms; Notations. The object M_o, the reference source S_p and the restitution source S_r may be real ($\rho > 0$), virtual ($\rho > 0$) at a finite distance or at infinity. Arrow f indicates the positive direction for θ.

It is sufficient to substitute these values into the general expression of the two restituted waves (expression II.12):

(II.14) $$\text{direct wave } A_1 = A_o A_p^* A_r$$

$$\text{conjugate wave } A_2 = A_o^* A_p A_r$$

in order to obtain the properties of the two images.

Let us determine A_o, A_p, and A_r by doing our reasoning for the point object M_o (Figure 10). Let C be the origin of the phases. Point M_o radiates to point P, of ordinate y, on H, the amplitude

(II.15) $$A_o = \exp\left[ik\left(r_o - \rho_o\right)\right] .$$

In triangle $M_o CP$ we have the following relation, keeping in mind the signs of θ_o, ρ_o, and r_o:

$$r_o^2 = \rho_o^2 + y^2 - 2\rho_o y \sin\theta_o ,$$

whence if $|\rho_o| \gg |y|$, and when θ_o is small,

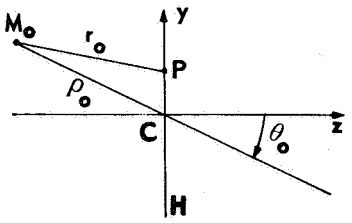

Figure 10.

(II.16) $$r_o - \rho_o = \left(y^2/2\rho_o \right) - y\theta_o$$

and (II.15) becomes

(II.17) $$A_o = \exp\left[ik\left(\frac{y^2}{2\rho_o} - y\theta_o\right)\right] .$$

Likewise the carrier gives on H

(II.18) $$A_p = \exp\left[ik\left(\frac{y^2}{2\rho_p} - y\theta_p\right)\right]$$

and the restitution wave

(II.19) $$A_r = \exp\left[ik\left(\frac{y^2}{2\rho_r} - y\theta_r\right)\right] .$$

In these expressions coefficient $1/\rho$ of $y^2/2$ is the curvature of the wave and θ is the angular coordinate of the center of curvature.

Substituting expressions (II.17) to (II.19) into (II.14), the two restituted waves may be written as follows:

Direct wave:

(II.20) $$A_1 = \exp\left\{ik\left[\frac{y^2}{2}\left(\frac{1}{\rho_o} - \frac{1}{\rho_p} + \frac{1}{\rho_r}\right) - y\left(\theta_o - \theta_p + \theta_r\right)\right]\right\} ,$$

Conjugate wave:

(II.21) $$A_2 = \exp\left\{ik\left[\frac{y^2}{2}\left(-\frac{1}{\rho_o} + \frac{1}{\rho_p} + \frac{1}{\rho_r}\right) - y\left(-\theta_o + \theta_p + \theta_r\right)\right]\right\} .$$

These waves converge to (or diverge from) their centers of curvature M_1 and M_2 which therefore are the restituted images. Coordinates ρ and θ of points M_1 and M_2 are given by

(II.22) $$\frac{1}{\rho_1} = \frac{1}{\rho_o} - \frac{1}{\rho_p} + \frac{1}{\rho_r}, \quad \frac{1}{\rho_2} = -\frac{1}{\rho_o} + \frac{1}{\rho_p} + \frac{1}{\rho_r} ,$$

(II.23) $$\underbrace{\theta_1 = \theta_o - \theta_p + \theta_r}_{\text{direct image } M_1}, \quad \underbrace{\theta_2 = -\theta_o + \theta_p + \theta_r}_{\text{conjugate image } M_2}.$$

These expressions are conjugation formulas analogous to those of lenses. They make it possible to determine the position of the direct image M_1 and that of the conjugate image M_2 defined by coordinates ρ_1, θ_1 and ρ_2, θ_2, as a function of the coordinates of the object M_o, of carrier S_p, and of the restitution source S_r.

If ρ_1 is positive, M_1 is real; if ρ_1 is negative, M_1 is virtual and the same applies to M_2. All combinations are possible for the two images, as we have already indicated above.

Furthermore we obtain formulas for the [angular] enlargement and [transverse] magnification of images M_1 and M_2.

(4) Angular Enlargement. To define this enlargement we must specify the position of the eye. We shall assume — and this is logical — that the eye is situated in the plane of the hologram. By differentiating (II.23) we obtain

(II.24) $$g_1 = d\theta_1/d\theta_o = +1, \quad g_2 = d\theta_2/d\theta_o = -1.$$

(5) Transverse Magnification. It is given by

$$\beta_{1,2} = d(\rho\theta)_{1,2}/d\left(\rho_o, \theta_o\right)$$

with ρ constant, or, keeping (II.24) in mind,

(II.25) $$\beta_1 = \rho_1/\rho_o, \quad \beta_2 = -\rho_2/\rho_o$$

(6) Axial Magnification.

(II.26) $$\alpha_1 = \frac{d\rho_1}{d\rho_o} = \left(\frac{\rho_1}{\rho_o}\right)^2, \quad \alpha_2 = \frac{d\rho_2}{d\rho_o} = -\left(\frac{\rho_2}{\rho_o}\right)^2.$$

From (II.26) it is inferred that, for a three-dimensional object, the direct image possesses a normal relief and the conjugate image an inverse relief.

(7) Change of Wavelength. If the recording of the hologram is carried out with wavelength λ and the restitution with wavelength λ', it is sufficient to substitute $k' = 2\pi/\lambda'$ instead of $k = 2\pi/\lambda$ into (II.19) in order to obtain the conjugation formulas:

$$(\text{II.27})\ M_1 \begin{cases} \dfrac{1}{\rho_1} = \dfrac{\lambda'}{\lambda}\left(\dfrac{1}{\rho_o} - \dfrac{1}{\rho_p}\right) + \dfrac{1}{\rho_r} \\ \theta_1 = \dfrac{\lambda'}{\lambda}\left(\theta_o - \theta_p\right) + \theta_r \end{cases} \qquad M_2 \begin{cases} \dfrac{1}{\rho_2} = \dfrac{\lambda'}{\lambda}\left(-\dfrac{1}{\rho_o} + \dfrac{1}{\rho_p}\right) + \dfrac{1}{\rho_r} \\ \theta_2 = \dfrac{\lambda'}{\lambda}\left(-\theta_o + \theta_p\right) + \theta_r \end{cases}$$

The enlargements and magnifications are simply multiplied by λ'/λ.

b. Extra-Meridian Conjugation Formulas

Points M_o, S_r, and S_p are now defined by coordinates ρ, θ, and φ (Figure 11).

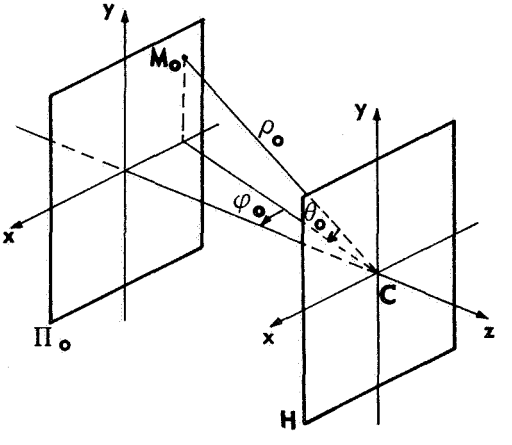

Figure 11. Configuration for the Extra-Meridian Conjugation Formulas.

By means of a reasoning similar to that used in Paragraph II.5.a we obtain conjugation formulas which are still the same as (II.22) and (II.23) for ρ and θ. To these are added the formulas containing φ:

$$(\text{II.28}) \qquad \varphi_1 = \varphi_o - \varphi_p + \varphi_r, \qquad \varphi_2 = -\varphi_o + \varphi_p + \varphi_r.$$

For the magnifications nothing has changed; as for the enlargements, they must be completed by the formulas containing φ:

$$(\text{II.29}) \qquad d\varphi_1/d\varphi_o = 1, \qquad d\varphi_2/d\varphi_o = -1.$$

Invariance of the Formulas. The position of origin C on the hologram has been chosen at random for establishing the conjugation formulas; hence the latter are invariant when C is displaced.

Likewise the origin axis of the θ's may be chosen at random. In particular, if instead of the z-axis we take the axis $S_r C$ of the restitution wave for origin (Figure 9), formulas (II.23) become even more simple:

$$\theta_1 = \theta_o - \theta_p, \quad \theta_2 = -\left(\theta_o - \theta_p\right). \tag{II.30}$$

c. The Aberration of Holograms

For the establishment of the conjugation formulas we have neglected, in expression (II.16), all the terms of an order higher than 2. This is comparable to the Gaussian approximation in classical optics. The higher-order terms represent the aberrations studied by various authors [9,11]. In this way one obtains the usual aberrations, spherical aberration coma, distortion, astigmatism, and "chromatic aberration" in the case of a change of wavelength on reconstruction.

We note that it is possible to obtain the conditions of rigorous stigmatism for the two images without long mathematical expansions. To this end we start from the rigorous expressions of the amplitude of the reconstructed waves which are, according to (II.14),

$$A_1 = A_o A_p^* A_r = \exp\left[i\left(\varphi_o - \varphi_p + \varphi_r\right)\right], \tag{II.31}$$

$$A_2 = A_o^* A_p A_r = \exp\left[i\left(-\varphi_o + \varphi_p + \varphi_r\right)\right] \tag{II.32}$$

(1) Direct Nonaberration Image. Let us take a point object M_o and its direct image M_1 (Figure 12). Stigmatism prevails if, regardless of the position of point P on the hologram, the optical path $\left(M_o P M_1\right)$ is constant, or, according to (II.31),

$$\left(\varphi_o - \varphi_p + \varphi_r\right) - \left(\varphi_o\right) = \text{Constant} \tag{II.33}$$

where φ_r, φ_p = constant, which entails, save for a constant factor,

$$A_r = A_p, \tag{II.34}$$

(II.35) $$A_1 = A_o.$$

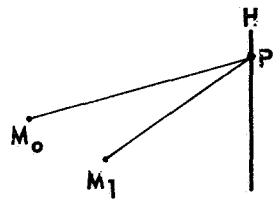

Figure 12. Rigorous Stigmatism. M_o is the object; M_1 the image. The condition of rigorous stigmatism is, according to Fermat's principle: $M_o P M_1$ = constant.

Hence rigorous stigmatism prevails if the reconstructed wave is identical to the reference wave; the latter can be a deformed wave taken at random. Then the image is identical to the object and is situated in the same region.

In the special case of a spherical reference wave originating from a point source S_p, the condition of stigmatism is that the point reconstruction source S_r must be identical with S_p.

(2) Conjugate Nonaberration Image. In the same manner we find that, if

(II.36) $$A_r = A_p^*,$$

the conjugate image is stigmatic. Moreover, (II.32) is then written as

(II.37) $$A_2 = A_o^*.$$

These formulas signify (Figure 13) that the nonaberration conjugate image O_2, the corresponding reconstructed source S_{r2} and the same elements relating to the direct image are symmetrical with respect to H.

Thus if S_{r1} is real, S_{r2} is virtual, and vice versa, and the same applies to the images.

d. Conclusions Regarding the Production of Holographic Images

The conjugation formulas immediately give a number of general rules, the most important of which are cited below:

(1) Angular Dimensions of the Images. According to (II.24), regardless of the operating conditions, the two images are seen from a point C of the plane of the hologram at an angle that is always constant, which is that at which the object is seen from the same point.

(2) Position of the Images in Space. According to (II.30), if we take axis CS_r of the reconstructed wave as the origin of the angles, the

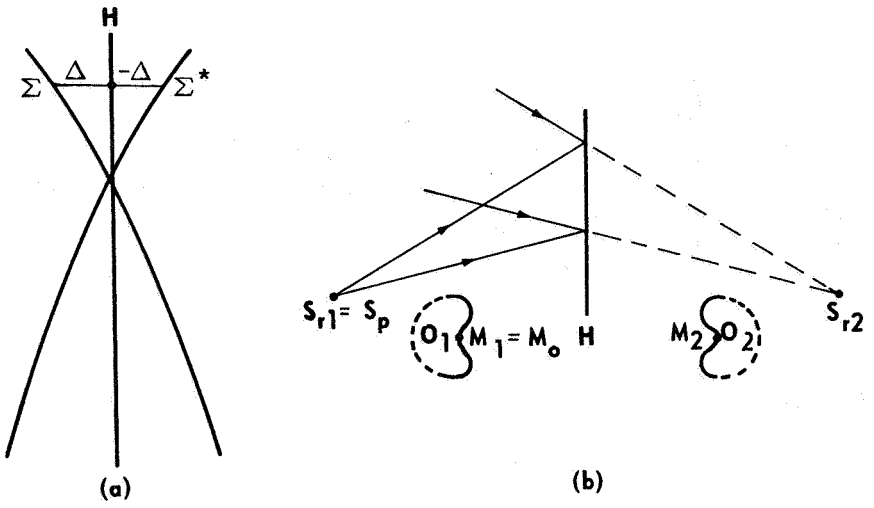

Figure 13. (a) Conjugate waves. Two conjugate luminous distributions A and A*, on H, correspond to two waves Σ and Σ^* which are symmetrical to H because to go from Σ to Σ^* one simply changes the sign of the path difference Δ. (b) The nonaberrant positions. (1) Direct image M_1: the reconstruction source S_{r1} must be identical with reference source S_p; then image M_1 coincides with object M_o. (2) Conjugate image M_2: restitution source S_{r2} is symmetrical to S_p with respect to H. The conjugate image is then symmetrical to the object.

directions of the two images M_1 and M_2 become

(II.38) $$\theta_1 = \theta_o - \theta_p, \quad \theta_2 = -\theta_1.$$

Consequently these two directions are symmetrical relative to the reconstructed axis (Figure 14) and are invariably linked to the latter by angle $\theta_o - \theta_p$ between the carrier and the object, defined during the recording. Hence,

a) If the reconstruction source turns by an angle α, the two images turn by the same angle;

b) If the hologram turns by an angle α, the images remain fixed in space.

(3) Plane Reference and Reconstructed Waves. In (II.22) we write $\rho_p = \rho_r = \infty$, whence

(II.39) $$\rho_1 = -\rho_2 = \rho_o .$$

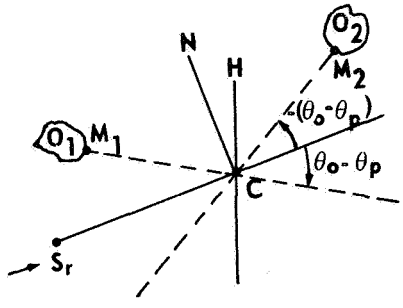

Figure 14. Position of the Images in Space.

The two images are linked in an invariable manner to the restitution axis S_rC by the angle between carrier and object, $\theta_o - \theta_p$, defined at the time of the recording.

If the reference wave and the reconstructed waves are plane, the direct image O_1 is identical to the object, and the conjugate image is deduced from O_1 by symmetry relative to a plane whose trace is the CN normal to S_rC.

Hence, according to (II.38), the two images are symmetrical with respect to a plane whose trace on Figure 14 is the normal CN to the reconstructed axis.

(4) Limitations of the Formulas (Bragg's Effect). One of the limitations of the use of the conjugation formulas is due to the aberrations. Another limitation is of a physical nature. In effect the emulsion is not infinitely thin as has been assumed until now. Its thickness is finite, of the order of 15 μ in the case of the Kodak 649F plates.

Thus the plate records the state of interferences not on a plane but in the volume occupied by the gelatin. We then obtain silver layers which constitute a three-dimensional network.

During the reconstruction this network presents an effect which is more directional when the fringes are closer to one another and more inclined in the emulsion.

Hence if during the recording $\theta_o - \theta_p$ and $(\theta_o + \theta_p)/2$ are small, the events taking place conform to the formulas, but when these angles are large, the diffracted amplitude rapidly decreases when θ_r deviates from θ_p and the image disappears.

Example. For the hologram of Figure 19, we had $\theta_o - \theta_p \simeq 35°$; if the reconstructed wave θ_r deviates by ±10° from angle θ_p of the carrier, the diffracted intensity drops to 10 percent of the maximum value obtained for $\theta_p = \theta_r$.

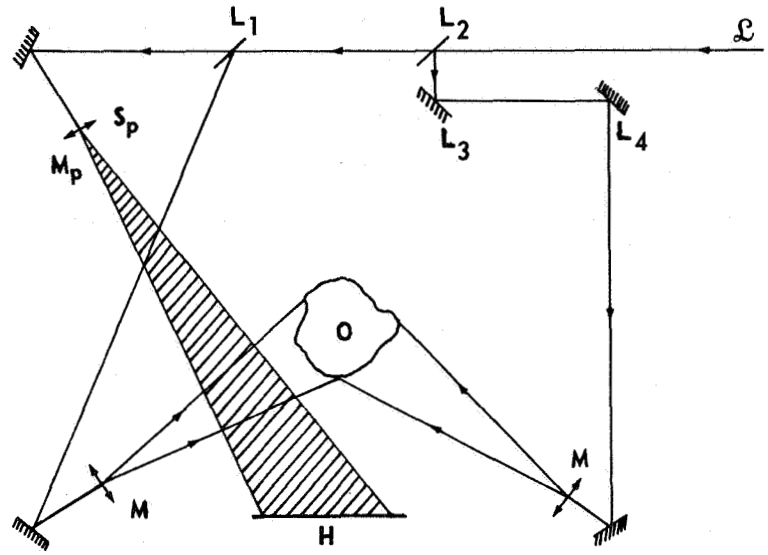

Figure 15. Assembly for the Recording of Holograms, with Two Illuminating Beams. The beam originating from a laser £ is divided into three parts by plates L_1 and L_2. Two of the beams serve for illuminating the object O, and the third (cross-hatched) constitutes the reference wave. All the beams are dilated by the lenses of microscope M in such a way as to cover plate H and the object. The reference source is then the focus S_p of objective M_p.

Furthermore, for $\theta_r \simeq \theta_p$, the conjugate image is extremely weak; to observe it, it is necessary to give θ_r a value close to θ_o.

6. Experimental Study of the Holograms

This paragraph deals with three-dimensional holograms. Interferential holography is studied in Paragraph II. 7. The two-dimensional Fourier holograms will be examined in Chapter IV.

a. The Assemblies

(1) Recording. The assemblies using parallel light exhibit a disadvantage of a practical nature: the beams are produced by collimators which are bulky and, in addition, the two-dimensional waves cannot be filtered from their heterogeneities. Hence we have used the assembly using divergent light, as shown in Figure 15.

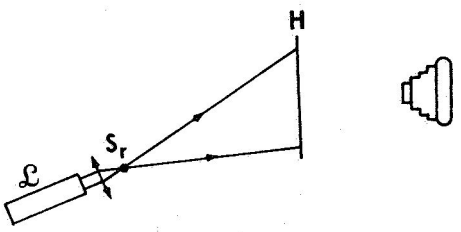

Figure 16. Reconstruction Assembly. The hologram is illuminated by a monochromatic point source S_r produced by laser £.

Similar assemblies have been used with one, two, or three illuminating beams.

(2) Reconstruction. The reconstruction takes place visually or photographically as in Figure 16; point S_r is in a position close to that of point S_p of Figure 15, in order to prevent aberrations. Figure 17 shows the whole restitution assembly: the image which appears in the hologram is that of the radar, shown also in Figures 21 through 23.

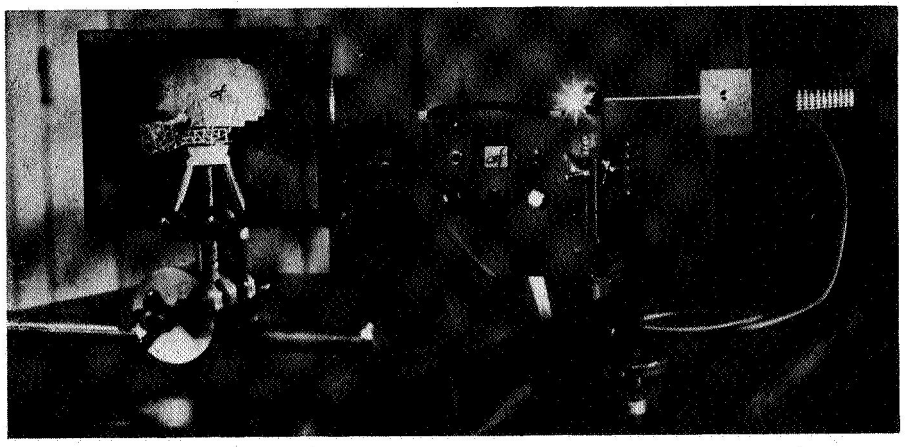

Figure 17. The Reconstruction Assembly. The image which appears in the hologram is that of the radar shown also in Figures 21 through 23.

Figure 18. Effect of Field Depth. The camera is focused on the foreground of the reconstructed image. The church in the background is blurred (Figure 19).

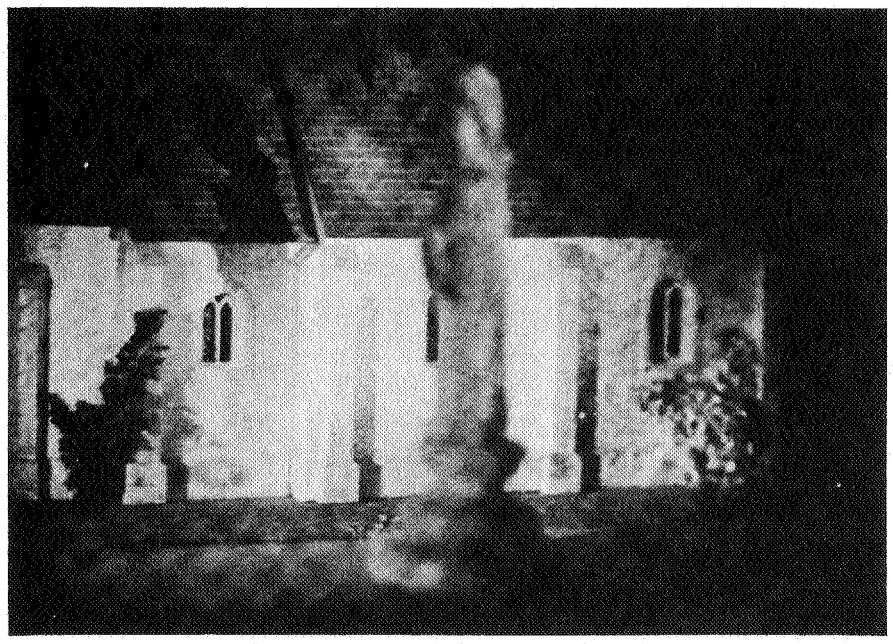

Figure 19. Effect of Field Depth. The camera is focused on the stained-glass window and the shadow of the statue; only this part of the church is in sharp focus. The statue in the foreground is completely blurred (Figure 20).

Figure 20. Effect of Field Depth. The lens of the camera is stopped down to a diameter which is smaller than that of the eye; the whole scene is in sharp focus, but we note, in an accentuated manner, the granulation which is characteristic of diffusing objects illuminated by a laser and observed visually.

For the reconstruction of Figures 18 and 19, the diaphragm of the lens was more open (30 mm), the granulation disappeared, and so did the depth of field.

b. Results

Figures 18 through 26 show the reconstructions, obtained from holograms, of a number of three-dimensional objects. Note, in particular, the parallax effect and the effects of the depth of field.

c. Experimental Conditions

The principal factors which influence the quality of holograms are the resolving power of the plates, the coherence length of the laser, the ratio between the amplitudes of the diffracted light and the carrier, and the mechanical stability of the recording arrangement.

(1) Resolving Power of the Plates. The photographic plate must record the microfringes of interferences which are formed in its plane (Figure 27).

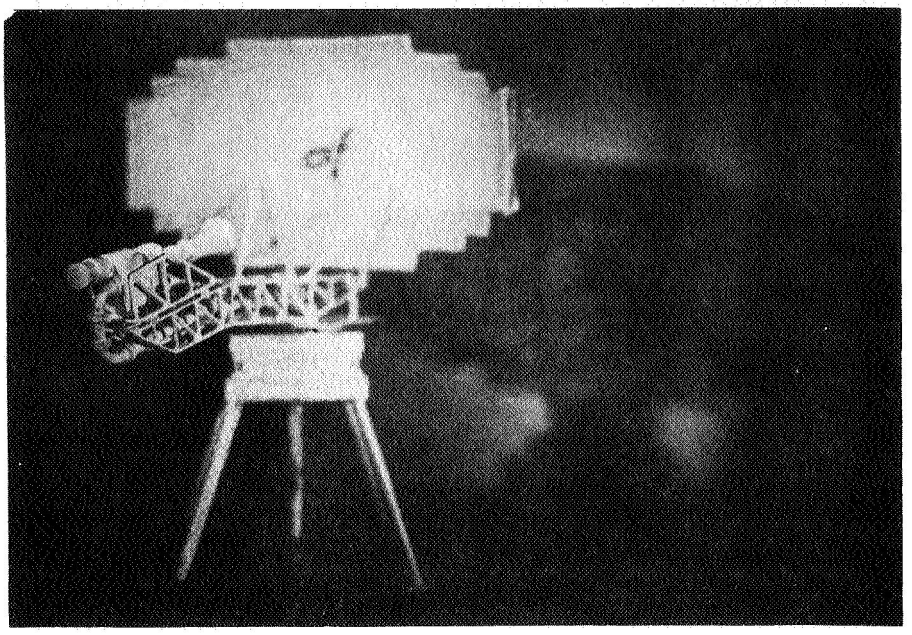

Figure 21. Effect of the Depth of Field. Focusing on the 'horn' of the radar, on reconstruction (Figure 22).

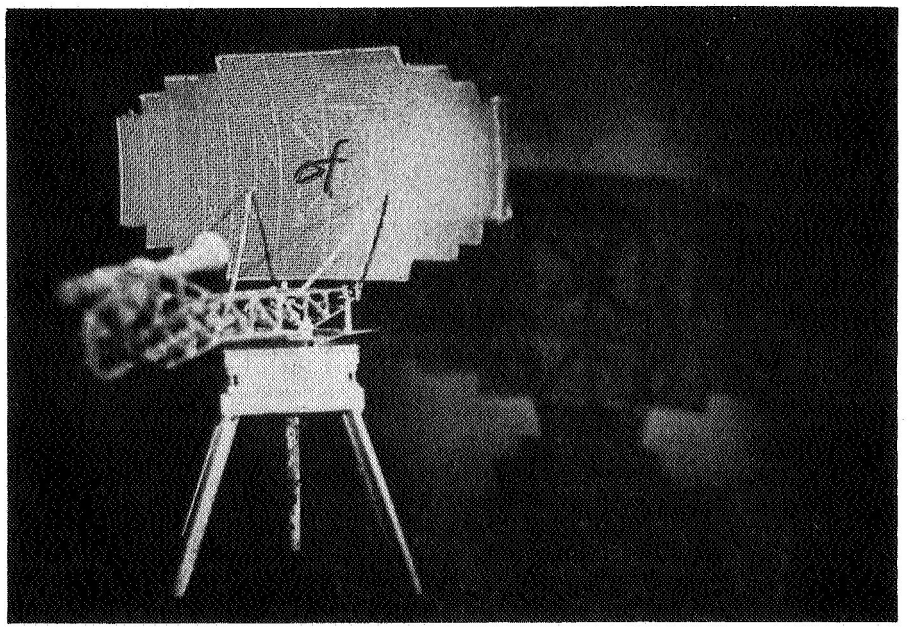

Figure 22. Depth of Field Effect. Focusing on the parabola of the radar (Figure 23).

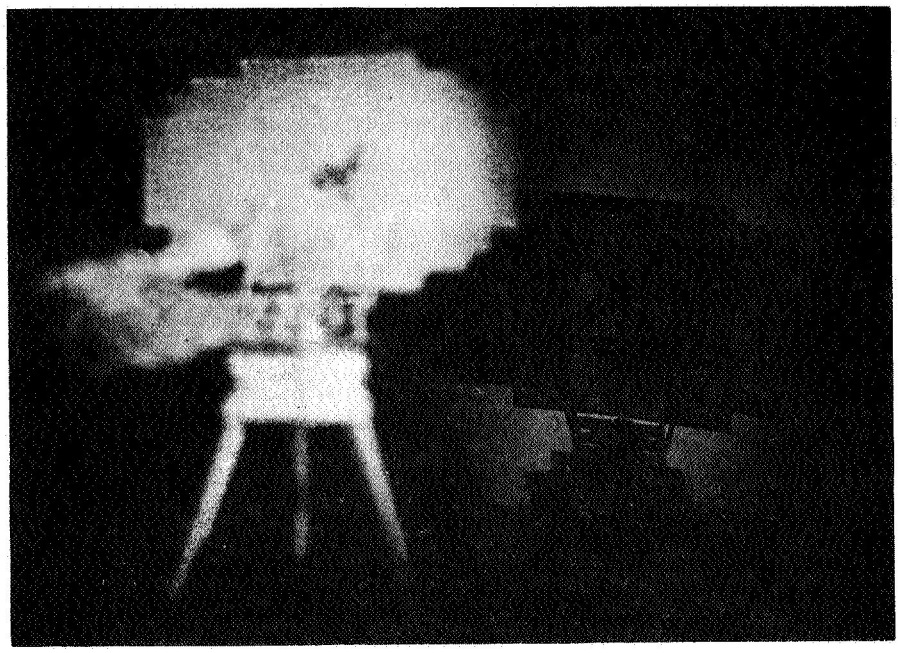

Figure 23. Depth of Field Effect. Focusing on the shadow of the radar antenna.

An exact study of the conditions under which the fringes are recorded requires the knowledge of the modulation transfer curve of the emulsion. This is generally not too well known. However, it is possible to do an approximate reasoning by means of which the orders of magnitudes are fixed.

Let us consider two plane waves Σ_o and Σ_p originating from the object and from the reference wave, respectively (Figure 28). Let us assume that Σ_o and Σ_p are inclined to hologram H by angles $+\alpha$ and $-\alpha$. The hologram is then formed of parallel fringes whose interfringe

$$\Delta y = \lambda/2 \sin \alpha \tag{II.40}$$

must be resolved by the emulsion.

Example. $\alpha = 30°$, which is a common case; $\Delta y = \lambda$. The resolving power of the plates should be close to the wavelength of the light. In practice for $\lambda = 6328$ Å (helium-neon laser) Kodak 649F plates are used, which resolve more than 2000 lines per mm.

(2) The Coherence Length of the Laser. This limits the depth of the objects which may be recorded. In effect, let A and B be the extreme

points of the object (Figure 29), assumed to be illuminated according to the direction of the arrow.

Then the path difference, relative to the carrier, cannot be equalized better than to within ± D. Hence it is necessary that the coherence length of the laser be greater than 2D.

The so-called "monomodal" lasers actually possess several axial modes. The 3-mW helium-neon laser, which has served for the preparation of the holograms of Figures 17 through 26, had a cavity length of $l = 75$ cm, which corresponds to an intermode distance $\Delta\nu = c/2l = 200$ MHz. In actual practice we have observed, as a result of beats, 3 modes, whence $2D = c/3\Delta\nu = 50$ cm.

For long exposures, however, it is prudent to take into consideration the whole width of the Doppler ray, or 1000 MHz.

Note that in Fourier holography, the path differences are small and no special precaution must be taken when using the laser.

(3) Amplitude of the Reference Wave. The photographic emulsions are generally not linear, which means, in the case of holography, that if the hologram receives (Paragraph II. 3) an illumination

$$I = |A_o|^2 + |A_p|^2 + A_o A_p^* + A_o^* A_p \qquad \text{(II. 41)}$$

its transmission factor in amplitude is not proportional to (II. 41) but to

$$t = I^{-\gamma/2}. \qquad \text{(II. 42)}$$

This expression may be expanded if

$$\left|A_o/A_p\right| \ll 1; \qquad \text{(II. 43)}$$

it becomes, when only the first terms are retained,

$$t = 1 - \frac{\gamma}{2}\left|\frac{A_o}{A_p}\right|^2 - \frac{\gamma}{2}\frac{A_o A_p^*}{|A_p|^2} - \frac{\gamma}{2}\frac{A_o^* A_p}{|A_p|^2} + \ldots \qquad \text{(II. 44)}$$

Physically this is the equivalent of choosing, on the blackening curve, an operating point determined by $|A_p|^2$, and of modulating the curve by $|A_o|^2$ over a short length.

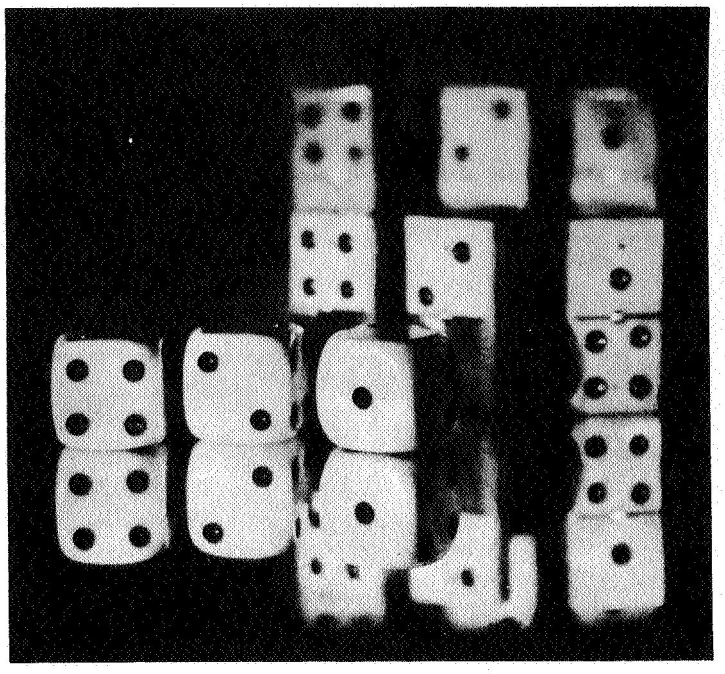

Figure 24. Parallax Effect. This figure is the reconstruction of a set of dice and dominoes placed on a mirror. The images of the objects in the mirror are also reconstructed and can be differentiated from the object by their split appearance. In effect the mirror employed is silvered on its back, and furnishes two images. Focusing on the foreground (Figure 25).

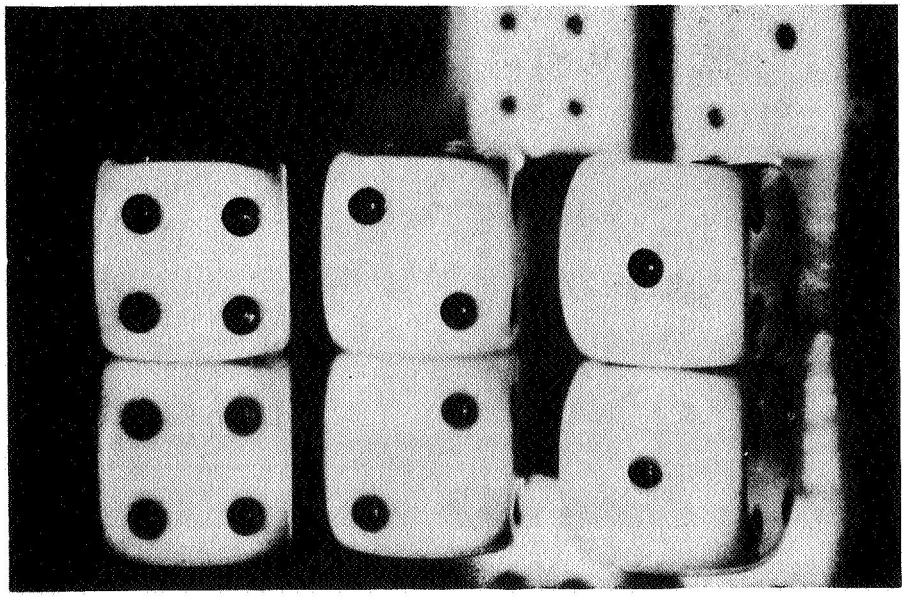

Figure 25. Parallax Effect. Enlarged detail of Figure 24; the lateral faces of the dice on the left are not visible (Figure 26).

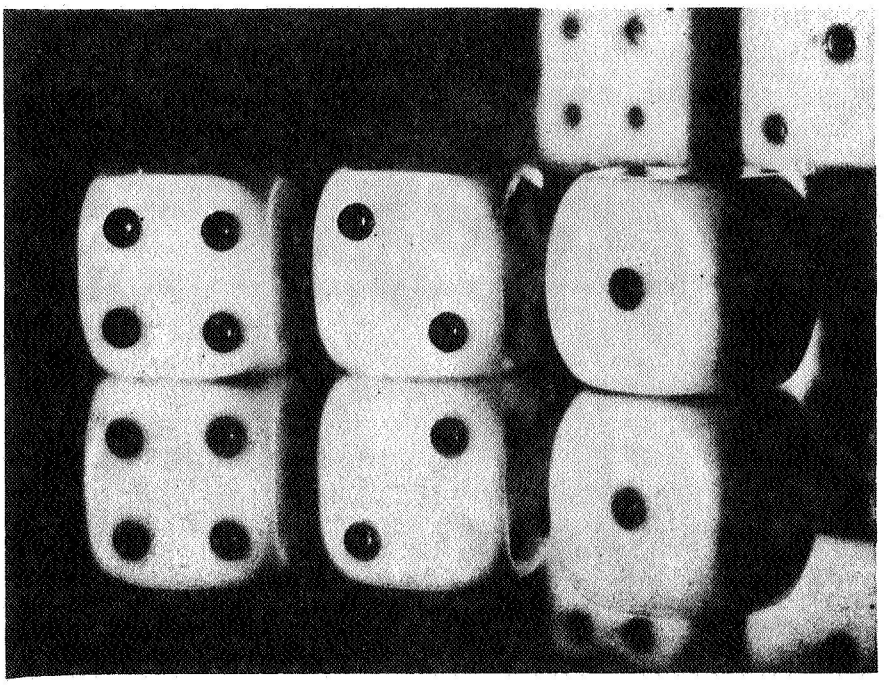

Figure 26. Parallax Effect. The camera was displaced to the right, the faces hidden in Figure 25 appear; the blurred dominoes in the background are also displaced.

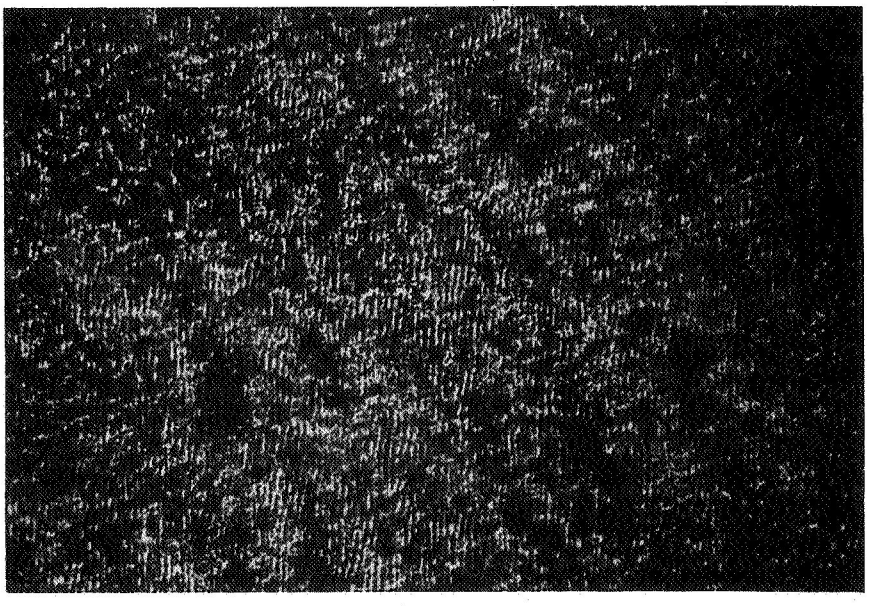

Figure 27. Photomicrogram of a Hologram. The interval between the interference fringes is of the order of 1 μ for this hologram.

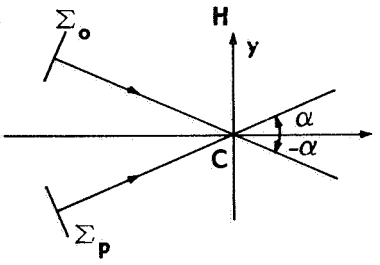

Figure 28. Two plane waves Σ_o and Σ_p inclined to plane H of the hologram by angles α and $-\alpha$, produce on H interference fringes spaced $\Delta y = \lambda/2 \sin \alpha$ apart.

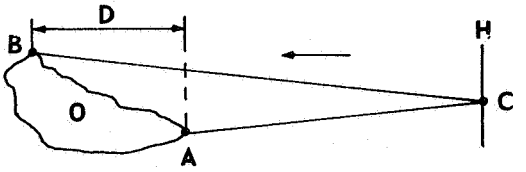

Figure 29. Influence of the Coherence Length of the Laser. If object 0, illuminated by a laser in the direction shown by the arrow, is recorded by holography in plane H, the coherence length of the laser must be greater than 2D.

If condition (II. 43) is not satisfied, terms of a higher order of the type

$$(II.45)\quad -\frac{\gamma}{2}\left(-\frac{\gamma}{2}-1\right)\cdots\left(-\frac{\gamma}{2}-n\right)\frac{1}{n!}\left[\left|\frac{A_o}{A_p}\right|^2+\frac{A_o A_p^*}{|A_p|^2}+\frac{A_o^* A_p}{|A_p|^2}\right]^n$$

appear, which have two principal effects:

a) They yield images of a higher order, like the ordinary networks. However, in view of the Bragg effect, these images disappear when the angle between the carrier and the diffracted light is large.

b) They change the distribution of the amplitudes in the two waves of the first order: the direct wave and the conjugate wave. This latter effect is not very pronounced in the three-dimensional holograms where the observation is often visual. Nevertheless in spatial filtering where the hologram is made to fulfill a mathematical function (Chapter IV), the result can be damaging. It is necessary in this case to respect condition (II. 43).

(4) Mechanical Stability of the Holographic Arrangement. The recording of a hologram consists, in fact, in arranging a photographic plate in the plane of an interferogram, in order to fix the latter. It is then necessary, especially if the exposure times are long, to take certain precautions in order to ensure the mechanical stability of the assembly.

Let us use the example mentioned in Paragraph II. 6. c: the interfringe interval in the hologram was less than 1 μ: hence the production of a translation of the fringes of the order of 1 μ, produced by the displacement of a single element of the recording device, is sufficient to make the hologram blurred. To be sure, to obtain a high hologram quality it is necessary that the displacement or

the deformation of the fringes under the influence of mechanical vibrations or thermal effects be very much less than 1μ, still referring to the above mentioned example.

The installation of an antivibration support made of concrete, shown in Figure 42, has made it possible to avoid these effects.

7. Interferometric Holography in Diffuse Light

a. The Method

The proposed method [12] makes it possible to prepare, by holography, an interferometer of the Mach-Zehnder type of a phase object, the latter being recorded through a diffusing screen.

To this end the following two operations are carried out in either order:

1) By means of the assembly of Figure 30 the hologram H of a polished glass D illuminated by a point source M is registered. The carrier is emitted from point S_p;

2) Without changing the assembly, the phase object O to be studied (Figure 31) is introduced in front of the polished object, and the image of the hologram of object O seen through the polished glass is prepared on the same emulsion.

On reconstruction, the hologram on which two images have been prepared reconstitutes an interferogram, an example of which is given by Figure 32 relative to a sheet of glass which exhibits "grains" and shows variations of thickness and of refractive index.

It may appear surprising that this could be done through a diffusion screen; however, the explanation of the phenomena is simple.

(1) Recording. In the first phase, point M gives on polished surface D the amplitude

(II. 46) $a;$

The polished object transmits (L is a linear operator)

(II. 47) $L(a)$.

In effect the polished object does not destroy the coherence of the light, since its thickness is small compared with the coherence length of the laser. Moreover Maxwell's equations are linear and the diffuser is passive, hence the action

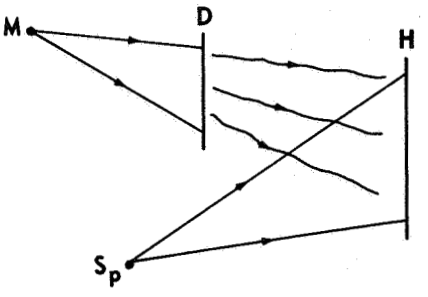

Figure 30. Interferential Holography in Diffuse Light. First operation: The hologram of the polished glass D illuminated by the point source M is recorded on H. So is the reference source.

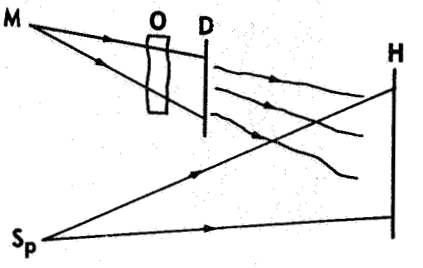

Figure 31. Second operation: Without changing the assembly of Figure 30, the phase object O to be investigated is introduced between source M and the polished glass D, and the image of the hologram of O is prepared on the same emulsion. Thus the hologram of O is recorded through the polished glass (Figure 32).

of the diffuser on the distribution (II. 46) is reflected by an unknown operator, because it depends on the nature of the diffuser; however, it is linear. Whence (II. 47).

Distribution (II. 47) gives, on the plane H of the emulsion (expression I. 9) the amplitude

(II. 48) $$A_1 = L(a) \bigstar d,$$

where $\bigstar$ signifies convolution and d is the normal derivative of Green's function relating to the diffraction (Fresnel's function in first approximation).

The carrier wave gives, on H, the amplitude

(II. 49) $$A_p.$$

The hologram records the illumination

(II. 50) $$E_1 = |A_1 + A_p|^2 .$$

In the second phase, the object O introduces the phase difference φ, and (II. 46) becomes

(II. 51) $$a\, e^{i\varphi} .$$

Figure 32. Interferential Holography in Diffuse Light. The hologram recorded according to Figures 30 and 31 reconstitutes an interferogram of the phase object O which has been recorded. In this case the object is a glass plate whose 'grains' and whose variations of refractive index and thickness are visible. The hologram obtained in this manner shows all the properties of the ordinary holograms in diffuse light, in particular, the interferogram is directly visible to the naked eye.

Hence (II. 48) becomes

(II. 52) $$A_2 = L(a\, e^{i\varphi}) \bigstar d$$

and the illumination (II. 50) becomes

(II. 53) $$E_2 = \left|A_2 + A_p\right|^2 .$$

The total illumination, due to the two operations, is

(II. 54) $$E_1 + E_2 = |A_1|^2 + |A_2|^2 + 2\left|A_p\right|^2 + (A_1 + A_2)\, A_p^* + (A_1^* + A_2^*)\, A_p .$$

(2) Reconstruction. Under the normal conditions of recording, the transparency t of the hologram (II. 54) is, according to expression (II. 10) in which γ has been standardized at -2

$$t = 1 + (A_1 + A_2)\, A_p^* + (A_1^* + A_2^*)\, A_p . \tag{II. 55}$$

If (II. 55) is illuminated by the reconstructed wave $A_r = A_p$, the second term, which reconstitutes the direct image, becomes

$$A_1 + A_2 \tag{II. 56}$$

or, keeping in mind (II. 48) and (II. 52),

$$\left[L(a) + L\left(a\, e^{i\varphi}\right)\right] \bigstar d \tag{II. 57}$$

or, since operator L is linear,

$$L\left[a\left(1 + e^{i\varphi}\right)\right] \bigstar d . \tag{II. 58}$$

This expression means that the reconstructed wave originates from the fictitious object

$$L\left[a\left(1 + e^{i\varphi}\right)\right] \tag{II. 59}$$

which represents, physically, the projection, on the polished object, of the interferogram $a\left(1 + e^{i\varphi}\right)$ of the dephasing object.

b. Properties of Interferometric Holograms in Diffuse Light

These are analogous to those of the usual holograms of diffusing objects. The grains or grooves of the emulsion are practically without effect on the quality of the interferogram. Moreover, to reconstruct the latter in its entirety it is sufficient to use any given part of the hologram. In actual practice 1 cm^2 gives very convenient results. Finally the image may be observed by the eye directly.

It may be noted that this is not the case in the methods using directed light [13,14]: the reconstruction can be accomplished only by means of an optical system which entirely covers the surface of the hologram, since the area of the reconstructed image is directly proportional to that of the hologram used.

8. Reproduction of Holograms

We shall conclude this chapter by discussing the important problem of the reproduction of holograms. This is beset with great practical difficulties [15]. In fact the interference fringes recorded in a hologram frequently have a spacing of the order of 1000 lines per millimeter; hence it is impossible to use optical systems for reproduction. Moreover, these fringes constitute a three-dimensional network (Paragraph II.5.d) which rules out reproduction by contact printing.

The process of coherent duplication proposed herein consists in using the beam directly transmitted during the reconstruction of a hologram H as the reference beam for a second hologram H', the object for H' consisting of the images of H.

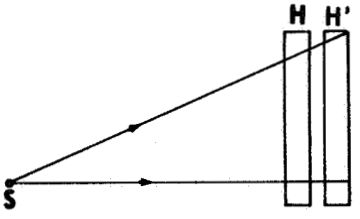

Figure 33. Coherent Copy of a Hologram H. When a plate H' is used for the preparation of an image as shown on the figure, with S representing a coherent source of any given position, a hologram H' is obtained which is an identical copy of the original, including the structure of the three-dimensional network recorded in the depth of the gelatin.

Let us consider (Figure 33) a hologram H whose transparency in amplitude is, according to (II.10),

$$t = 1 - \frac{\gamma}{2} A_o A_p^* - \frac{\gamma}{2} A_o^* A_p . \qquad \text{(II.60)}$$

This hologram is reconstructed by illuminating it with wave A_p; it then transmits the amplitude distribution

$$A_i = t A_p . \qquad \text{(II.61)}$$

Plate H' placed behind hologram H records the intensity

$$I = |A_i|^2 \qquad \text{(II.62)}$$

and its amplitude transparency

$$t' = I^{-\gamma/2} \qquad \text{(II.63)}$$

becomes, using the same approximations as those which led to (II.60),

$$t' = 1 + \frac{\gamma^2}{2} A_o A_p^* + \frac{\gamma^2}{2} A_o^* A_p . \qquad \text{(II.64)}$$

Except for some constants, this expression is the same as (II. 60); hence we have obtained a copy of hologram H. The quality of the reconstructed image is practically identical to that of the original, and the degradation due to the fact that the copy registers, in addition to its own background, that of the original as well, is not perceptible to the eye.

It is shown, moreover, that plates H and H' need not be in contact, and that the copying wave may be chosen at random, as long as it is coherent and originating from a point source.

9. Conclusions on Holography

Holograms have two main functions:

a) They permit the recording, on a photosensitive material, of both the amplitude and the phase of a coherent light wave;

b) They permit the summate in phase and amplitude several coherent waves recorded successively.

The first property makes the hologram a remarkable data storage system while the second represents a veritable data-processing operation.

In this chapter we have listed a number of other properties and applications of holograms, but have reserved the applications to the filtering of spatial frequencies. The fact of being able to record an optical wave representing a complex function, e.g., a Fourier transform, permits one, in effect, to obtain photographic transparencies which may act as complex filters in coherent optical filtering.

Thus it is possible to develop certain applications of this method which had existed only potentially before the discovery of holograms. This will be discussed in Chapter IV.

III. FILTERING OF SPATIAL FREQUENCIES

1. The Possibilities Inherent in the Method

Ever since its discovery in 1953 [1], the filtering of the spatial frequencies in coherent light has been considered for a number of applications aimed, in particular, at the improvement of optical images [5-7, 16].

This method has acquired an increased significance at the present time as a result of the new prospects which are opening up for this method in the optical treatment of data. This situation is due to several factors:

a) Theoretical possibilities. A coherent optical system establishes between three functions of two variables — the signal $f(x,y)$, the percussional response $h(x,y)$ of the system, and the response $r(x,y)$ to the signal — a very general linear correspondence: a convolution relation.

Now a number of mathematical operations are but special cases of convolution, notably the integration, differentiation, correlation, self-correlation or the scalar product of two functions;

b) Experimental possibilities. All these operations may be effectively carried out (as we shall see some examples of this in Chapter IV) not only for real and positive functions but also for complex functions.

Experimentally, the operator "convolution by $h(x,y)$" is applied to $f(x,y)$ in Fourier's space: this reduces simply to placing a filter into the spectral plane of the optical system.

The gas laser and the holograms which permit the recording of complex functions greatly facilitate the realization of some of these filters or the material representation of complex functions.

In this chapter we summarize the aspects of optical filtration which will be used later on, and give an example of application which may serve for the treatment of the photographic plates of bubble chambers.

2. The Mathematical Bases of Optical Filtering

Optical filtering in coherent light may be justified by purely mathematical considerations.

In effect, the problem consists in finding the law of correspondence between a two-dimensional signal $f\left(M_o\right)$ and the (filtered) response $r(M)$ given by an optical system defined by its percussional response $h(M)$.

To this end it is sufficient to assume that

(III.1)
- a) the transformation is linear;
- b) the percussional response $h(M)$ of the instrument is invariant by translation.

Condition (III. 1b) means that if the signal is Dirac's pulse $\delta(M_o)$, and if $\delta(M_o)$ gives the response $h(M)$, then the pulse $\delta(M_o - M_1)$, displaced by M_1 by translation, gives the response $h(M - M_1)$. It is shown [17,18] that conditions (III. 1) entail the law of correspondence.

(III. 2) $$r(M) = f(M) \ast h(M) \ .$$

This convolution product is written, after a Fourier transformation, as follows, with $R(\Omega)$, $F(\Omega)$ and $H(\Omega)$ being the Fourier transforms of $r(M)$, $f(M_o)$ and $h(M)$, and $\Omega(u, v)$ the general point in Fourier's space.

(III. 3) $$R(\Omega) = F(\Omega)\ H(\Omega) \ .$$

From this it is deduced that the correspondence between $f(M_o)$ and $r(M)$ is a linear filtering which follows the following scheme ($\otimes$ signifying multiplication):

(III. 4)

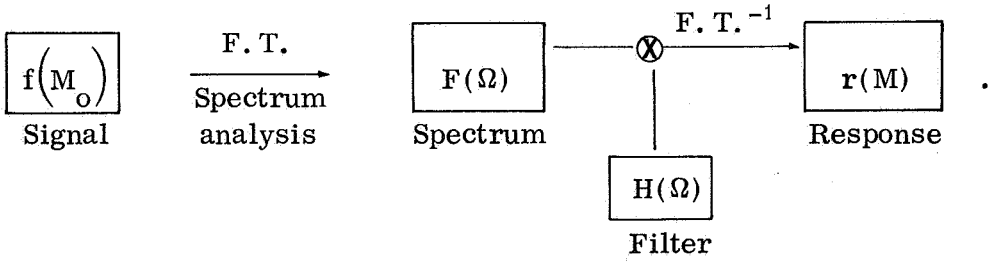

The preceding reasoning does not make use of any physical mechanism. It is applicable to the case of both coherent and of incoherent illumination, provided the conditions (III. 1) are satisfied. However, in incoherent illumination, the Fourier spectra $F(\Omega)$, $H(\Omega)$ have no physical meaning. The case is different in the case of coherent illumination: in that case the scheme of (III. 4) may be realized by double refraction.

3. Double Refraction

a. Process

The treatment (III. 4) may be carried out optically in a restitutor by double diffraction [18]. The signal produces, by means of a first diffraction, a Fourier spectrum which, when filtered, gives (restitutes) the response by means of a second diffraction.

In reality the signal gives, in the spectral plane, the product of the Fourier spectrum and a spherical phase term (Paragraph I. 4. a). To obtain a linear filtering, i. e., to accomplish the conditions (III. 1), it is necessary to compensate this factor. This may be done by a convenient arrangement of the optical system [19] (also Paragraph IV. 3. b).

Then it is possible to neglect the phase term in the filtering process [Note: The compensation is effective only at the end of the treatment process, in the plane of the response (image); hence when a holographic recording is made on the level of the spectral plane (Paragraph IV. 4. a), it will be necessary to take into account these terms which are recorded in the form of holographic lenses, with their aberrations.]

This process consists of three phases which will be recapitulated below; the proofs will be given in Appendix 1.

(1) The Restitutor. This consists of an object plane (signal) Π_o, a spectral plane $\mathcal{F}$, and a response plane (image plane) Π (Figure 34).

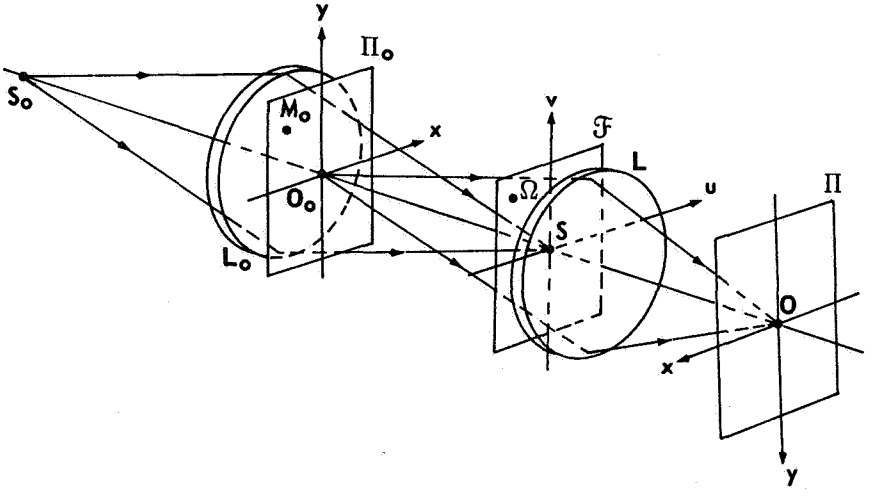

Figure 34. The Restitutor Operating by Double Diffraction. Object f M_o is arranged in plane Π_o; it is illuminated by the convergent beam originating from lens L_o and gives by means of a first diffraction, in plane $\mathcal{F}$, the Fourier spectrum $F(\Omega)$. The latter is filtered by a filter $H(\Omega)$ situated in $\mathcal{F}$, and gives by means of a second diffraction, in plane Π, the image of Π_o through lens L, the filtered response $r(M) = f(M) \bigstar h(M)$.

The optical system consists, schematically speaking, of spectrum analyzer lens L_o and of a restitution lens L.

The signal to be filtered is generally recorded on a photographic emulsion whose transparency in amplitude t (Appendix 2) is proportional to signal $f(M_o)$.

(2) Spectrum Analysis. The signal $f\,M_o$ is placed in object plane Π_o having a general point $M_o(x_o, y_o)$. It is illuminated by a convergent beam originating from lens L_o.

The plane normal to the axis at the point of geometric convergence S of the beam is the spectral plane $\mathcal{F}$. The position vector in this plane is $P(x_1, y_1)$ or, in reduced coordinates (Paragraph I. 4. c),

$$\Omega(u, v) = P/\lambda d, \tag{III. 5}$$

where d is the distance between planes Π_o and $\mathcal{F}$, and λ the wavelength.

Under the effect of the convergent illumination, signal $f(M_o)$ diffracts a wave; the latter forms in plane $\mathcal{F}$ a luminous distribution which is the Fourier spectrum $F(\Omega)$ of $f(M_o)$.

$$f(M_o) \xrightarrow{F.T.} F(\Omega) \tag{III. 6}$$

save for a phase factor.

(3) The Filtering. A filter is placed in plane $\mathcal{F}$ whose transparency in amplitude is $H(\Omega)$. Actually, in a limiting case, this filter may be a simple aperture.

After passing through the filter the amplitude of wave $F(\Omega)$ becomes

$$R(\Omega) = F(\Omega)\ H(\Omega) \tag{III. 7}$$

b. Restitution

To ensure condition (III. 1) and to compensate the phase factor in (III. 6), the restitution lens L should have its entry diaphragm in the spectral plane $\mathcal{F}$. This is shown schematically on Figure 35 by a thin lens, placed in plane $\mathcal{F}$. The transverse magnification of L will be standardized at $\gamma = +1$.

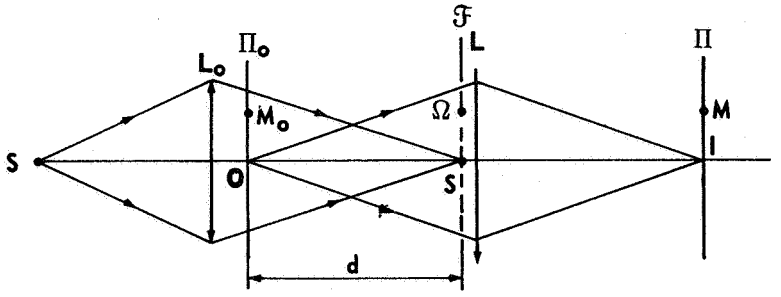

Figure 35. Restitutor Operating by Double Diffraction. To ensure the conditions of linearity and invariance by translation, the diaphragm of restitution lens L must be placed in the spectral plane $\mathcal{F}$.

After passing through L, the wave (III. 7) gives by means of a second diffraction the following response on image plane Π having a general point $M(x,y)$:

$$r(M) = \int_{\mathcal{F}} F(\Omega)\ H(\Omega)\ e^{2\pi i\, \Omega.M}\, d\Omega \tag{III. 8}$$

which is the inverse Fourier transform of the filtered spectrum:

$$F(\Omega)\ H(\Omega) \xrightarrow{F.T.^{-1}} r(M). \tag{III. 9}$$

Let $h(M)$ be the percussional response of filter $H(\Omega)$:

$$H(\Omega) \xrightarrow{F.T.^{-1}} h(M);$$

which represents, physically, the distribution of the amplitudes in the image of a point luminous object placed at the origin of plane Π_o.

Applying the convolution theorem to (III. 8) we then obtain

$$r(M) = f(M) \ast h(M) \tag{III. 10}$$

To sum up, we have:

$$\underset{\text{signal}}{f(M_o)} \xrightarrow{F.T.} \underset{\text{spectrum}}{F(\Omega)} \text{ — } \otimes \text{ — } \underset{\text{filtered spectrum}}{R(\Omega) = F(\Omega)\ H(\Omega)} \xrightarrow{F.T.^{-1}} \underset{\text{response}}{r(M) = f(M) \ast h(M)}. \tag{III. 11}$$

$$H(\Omega) \xrightarrow{F.T.^{-1}} h(M)$$

filter

4. Properties of Spatial Filtering

a. The Spatial Frequencies

The spectrum analysis correlates with each elementary sinusoidal component of the object $f(M_o)$ with point Ω of the spectral plane, and the amplitude of the light wave at this point is proportional to the amplitude to the elementary sinusoid.

In effect, let us take such a sinusoidal component $f(M_o)$ of period p, and a unit vector U (Figure 36) normal to the "lines" of the sinusoid. In a complex form we have

$$f(M_o) = a \exp\left(2\pi i \frac{U}{p} \cdot M_o\right). \tag{III.12}$$

We say that the spatial frequency of the object $f(M_o)$ is 1/p or, to take the orientation of the object into account, U/p.

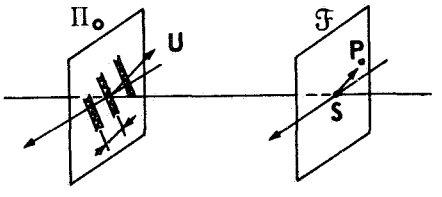

Figure 36. The Spatial Frequencies. The object $f(M_o) = a \exp\left[2\pi i (U/p).M_o\right]$, of spatial frequency 1/p, gives in spectral plane $\mathcal{F}$, a spectrum which, when $f(M_o)$ is unlimited, is a point P whose position in reduced coordinates is $\Omega = U/p$. If the object is not unlimited, this point is the center of a diffraction spot.

In the spectral plane we obtain the Fourier transform of (III.12)

$$F(\Omega) = a \int_{\Pi_o} \exp\left[2\pi i M_o \cdot \left(\frac{U}{p} - \Omega\right)\right] dM_o$$

which is the Dirac distribution $F(\Omega) = a\,\delta\left(\Omega - \frac{U}{p}\right)$. This represents a point with amplitude a and situated at $\Omega = \frac{U}{p}$, i.e., at a distance from the center of the Fourier plane which is equal to the spatial frequency 1/p.

Coming back to the simple coordinates in the spectral plane, with $P = \lambda d \Omega$ we have

$$F(P) = a\,\delta\left(\frac{P}{\lambda d} - \frac{U}{p}\right),$$

in other words a point of the spectral plane $\mathcal{F}$ situated at $P = (\lambda d/p)\ U$ whose distance from center S is proportional to the spatial frequency and to the distance d between planes Π_o and $\mathcal{F}$.

Thus the center of the spectral plane corresponds to the continuous component of the object and the edge at the high frequencies.

NOTE. If, instead of considering the expression (III.12), which is the result of a decomposition of the object into complex sinusoidal components, we had considered the real sinusoid $f(M_o) = 1 + \cos\left(2\pi \frac{U}{p} \cdot M_o\right)$, we would have obtained the frequencies $\Omega = 0$, corresponding to the continuous component, and $\Omega = \pm U/p$ corresponding to the decomposition of the cosine.

b. The Cutoff Frequency

If the filtering function $H(\Omega)$ reduces to a simple aperture (the entry diaphragm of L, of transparency 1 and of radius R or $R/\lambda d$ in reduced coordinates), it only permits the passage of spatial frequencies such as $|\Omega| = 1/p \leq R/\lambda d$. The spatial frequency $1/p = R/\lambda d$ is the cutoff frequency.

The period of the corresponding "cutoff" sinusoid is seen from the center S of plane $\mathcal{F}$ at an angle $\alpha = p/d = \lambda/R$, which is the classical "resolving power" (in coherent light) due to the diffraction. All the spatial frequencies such as $1/p < R/\lambda d$ are transmitted without alteration, since $H(\Omega) = 1$ in the diaphragm; the instrument is a low-pass filter with a flat band.

Below the attention is devoted to the data-treatment aspect and not to the power of resolution. Hence it will be assumed that all the useful frequencies are transmitted by the diaphragm.

This means, in particular, that if $H(\Omega) = 1$ we have (expression III.9):

$$r(M) - f(M).$$

The response is identical to the signal.

5. An Example of Application

To conclude this general part of the discussion it may be useful to give a simple example of optical filtering, which may find an application in the treatment of photographic plates of bubble chambers.

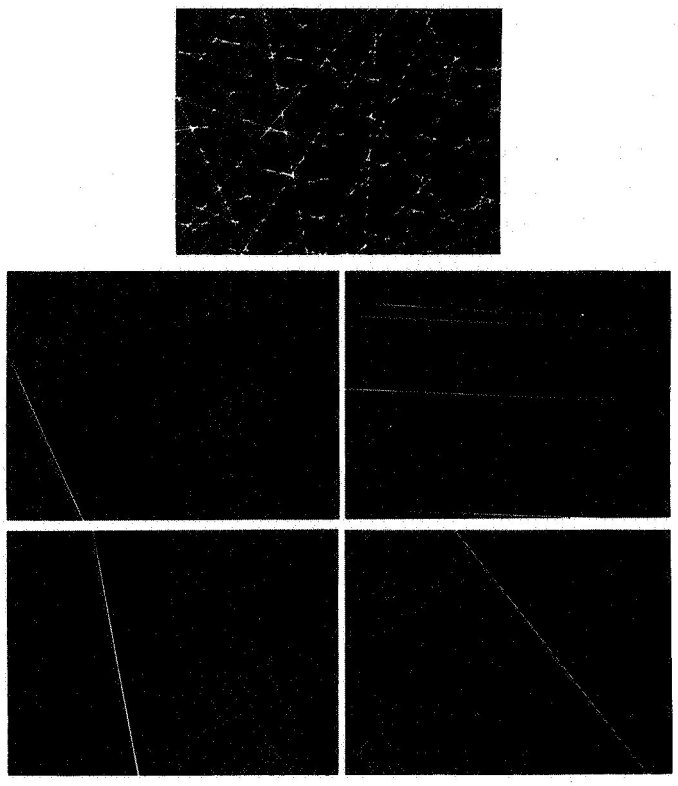

Figure 37. Extraction of Straight Lines by Optical Filtering. When the Fourier spectrum of the object (above) is filtered by a fine slit passing through the center of the spectral plane, there remain in the image plane of the restitutor only the straight lines normal to the slit. By turning the slit, all the lines of the object are successively extracted. By contrast, if the filter had consisted of an opaque line, the lines of the object normal to the filter would have successively disappeared.

These plates comprise essentially parallel traces produced by the exciting particles. It may be advantageous to "cleanse" the plate of these traces, or on the contrary, to bring them to light.

This can be done quite simply, because a long and fine straight line L gives, regardless of its position in the object plane, a spectrum concentrated on a line L' normal to L and centered on center S of the Fourier plane.

To eliminate L and all straight lines parallel to L, it is sufficient to eliminate L'; to ensure that only lines L will appear it is sufficient to allow only L' to pass through. Figure 37 shows the result obtained when a slit is rotated in the spectral plane: straight lines L normal to the slit successively appear in the image.

IV. PATTERN RECOGNITION BY FILTERING OF SPATIAL FREQUENCIES

1. Introduction

Pattern recognition consists in detecting the presence and localizing the position of a signal in the presence of other signals or in the presence of noise. An example of such a process is the identification of characters or words in a text.

It may appear that an optical self-correlation carried out on the signal would furnish a convenient means for accomplishing the identification.

However, the methods using self-correlation lead to ambiguities, and it frequently happens that the object identified is different from that sought.

To remedy these disadvantages a method has been proposed which is characterized by a low probability of false alarm [20, 21].

To this end the object to be treated (signal to be identified + noise) is subjected to a transformation which permits the survival of only the lines of discontinuity of the object, or more generally, the zones which exhibit a rapid variation of amplitude.

The object transformed in this manner is then correlated with a signal model which had undergone the same transformation; the result of this is an identification with a high signal/noise ratio.

The transformation is obtained by the use of suitable differential operators. The complete identification treatment and, in particular, the differentiation operations are easily carried out in coherent light on the basis of the properties of the Fourier transformation and of the filtering of spatial frequencies. It may be noted that this is a general method, and that it is just as easy to construct a filter leading to the identification of a complex object as a filter identifying a simple object.

2. Principle of Pattern Recognition

Let us consider a two-dimensional signal $s\left(M_o\right)$ in the presence of an additive noise $b\left(M_o\right)$. Using the notations of Chapter III, this corresponds to the object

$$f\left(M_o\right) = s\left(M_o\right) + b\left(M_o\right). \tag{IV.1}$$

The problem consists in detecting the signal in the object. This may be done by filtering the spatial frequencies according to the scheme of Paragraph III.2 as follows: (Note: When there is no ambiguity, the subscript "o" relating to the object will be dropped.)

(IV.2)

object	$f(M) = s(M) + b(M)$
	F.T. ↓
spectrum	$F(\Omega) = S(\Omega) + B(\Omega)$
	⊗ ← $H(\Omega)$ filter
filtered spectrum	$R(\Omega) = S(\Omega)\ H(\Omega) + B(\Omega)\ H(\Omega)$
	$F.T.^{-1}$ ↓
response	$r(M) = s(M) \bigstar h(M) + b(M) \bigstar h(M)$

Response r(M) of the system consists of two terms. The first term is the convolution product $r_s = s(M) \bigstar h(M)$, which is the response in Π due to signal s(M).

The second convolution product $r_b = b(M) \bigstar h(M)$ is the response due to the noise b(M).

In general, r_s and r_b are no longer images but distributions of luminous amplitude.

In actual practice, the identification of the signal s(M) consists in finding a filtering function $H(\Omega)$ which would furnish in the image plane Π (Figure 34) a distribution of illuminations $E = |r_s(M)|^2$ whose maximum E_m indicates, without ambiguity,

a) The presence of the signal in the object;

b) The position of the signal (Figures 38 and 47).

This implies that the signal/noise ratio must be sufficiently high.

It is possible to determine from scheme (IV.2) — without for the time being specifying $H(\Omega)$ — some general properties of pattern recognition.

a. The Signal/Noise Ratio

Let us assume that function $H(\Omega)$ has been determined. $H(\Omega)$ is the Fourier transform of the percussional response h(M) of the optical system [provided with filter $H(\Omega)$]:

$$h(M) \xrightarrow{F.T.} H(\Omega)$$

According to (IV.2) the response in plane Π is

$$r(M) = s(M) \bigstar h(M) + b(M) \bigstar h(M).$$

Let $|r_s|^2_m$ and $|r_b|^2_m$ be the maximum illuminations which correspond to these responses. The signal will be detected if $|r_s|^2_m > |r_b|^2_m$, or more precisely, if the signal/noise ratio

(IV.3) $$\rho = |r_s|^2_m / |r_b|^2_m$$

is sufficiently large so that the contrast $c = \left(|r_s|^2_m - |r_b|^2_m\right) / \left(|r_b|^2_m + |r_s|^2_m\right)$ can be measured. Figures 55 and 56 give examples of such measurements.

b. Automatic Positioning of the Response

The properties of (III.1) of linearity and invariance by translation have two consequences.

(1) Translation. The filter, designed for the recognition of signal $s(M)$, will also recognize the signal after a translation of M_1 in its plane; the response in plane Π is simply translated by the same quantity M_1 (Figure 38).

(2) Additivity. The sum of the signals, $\Sigma_n s\left(M - M_n\right)$, will give the response $\Sigma_n r_s\left(M - M_n\right)$.

Property (2) is obvious; property (1) can be readily proved.

Let us take a signal $s(M)$ situated, for the sake of convenience, in the center of the object plane (Figure 38).

Let δ be the Dirac distribution. We know that δ is the unit operator of the convolution.

Consequently, the response $r_s(M)$ to signal $s(M)$ (scheme IV.2) is written as $r(M) = s(M) \bigstar h(M) \bigstar \delta(M)$, which becomes, for the translated signal $s(M - M_1)$:

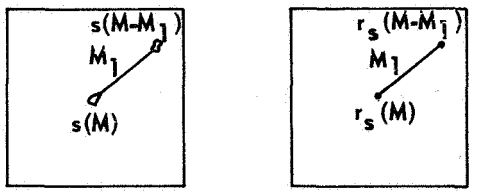

Figure 38. Automatic Positioning of the Response. In coherent optical filtering, for any given filter, it is deduced from the properties of linearity and invariance by translation of the percussional response of the optical system that a) a translation of the signal in the object plane produces the same translation of the response in the image plane; and b) the sum of n signals gives the sum of n responses.

$$r_1(M) = s(M - M_1) \bigstar h(M) \bigstar \delta(M)$$

$$= s(M) \bigstar h(M) \bigstar \delta(M - M_1)$$

$$= r_s(M - M_1)$$

or the translated response.

The physical meaning of this is clear.

The filtering process is written for the nontranslated signal $s(M)$:

a) spectrum analysis, $s(M) \xrightarrow{F.T.} S(\Omega)$;

b) filtering by $H(\Omega)$, $R(\Omega) = S(\Omega)\ H(\Omega)$

c) restitution, $R(\Omega) \xrightarrow{F.T.^{-1}} s(M) \bigstar h(M)$

and for the translated signal $s(M) - M_1$):

a) analysis, $s(M - M_1) \xrightarrow{F.T.} S(\Omega)\ \exp(-2\pi i\ \Omega.M_1)$;

b) filtering, $\underbrace{S(\Omega)\ H(\Omega)}_{R(\Omega)}\ \exp(-2\pi i\ \Omega.M_1)$;

c) restitution, $R(\Omega)\ \exp(-2\pi i\ \Omega.M_1) \xrightarrow{F.T.^{-1}} r(M - M_1)$.

This means that translation M_1 introduces, in the Fourier plane, a linear phase term containing M_1, which is preserved after filtering and which places the response in position.

Figure 52 gives an example of recognition by a filter designed for identifying the character "e": all the "e's" of the text are identified with their relative position.

3. The Self-Correlation Method

One method of approaching the problem of pattern recognition consists in optimizing the signal/noise ratio in the exit plane of the system. This leads to the theory of the adapted filter [22].

However the adapted filter can only operate correctly if the noise is not correlated with the signal, or is correlated only to a slight extent. Especially for the recognition of letters it is possible to obtain, in the case of similar shapes, a response that is more perceptible for the noise than for the signal sought.

It is only in certain limited cases that we obtain an indication of presence with a high probability. Nevertheless, it is necessary to discuss the method of self-correlation, because the adaptation of this method which we have made, notably by constructing hologram filters with low aberrations, will be useful in the differentiation method discussed in Paragraph IV.6. This method makes it possible to strongly decrease the probability of false alarm when the correlation between the signal and the noise is high.

The adapted filter. It is shown [16, 23] by a reasoning analogous to that used in radar technique for the treatment of temporal signals, that the two-dimensional filter which optimizes the signal/noise ratio in the search for a signal s(M) is proportional to

$$H(\Omega) = S^{*}(\Omega) / |B(\Omega)|^{2}, \tag{IV.4}$$

or the quotient of the conjugate complex of the Fourier transform of the signal and the spectral density of the noise.

In Paragraph IV.5 we shall show that function $1/|B(\Omega)|^{2}$ cannot be realized physically; hence we are led to the approximation

$$|B(\Omega)|^{2} = \text{constant} \tag{IV.5}$$

and filter (IV.4) becomes

$$H(\Omega) = S^{*}(\Omega) \tag{IV.6}$$

which gives the percussional response

$$H(\Omega) \xrightarrow{F.T.^{-1}} s^{*}(-M); \tag{IV.7}$$

hence if, in response $r_s(M) = s(M) \bigstar h(M)$ due to the signal (scheme IV.2), we substitute $S^*(-M)$ into $h(M)$, we obtain

(IV.8) $$r_s(M) = s(M) \bigstar s^*(-M)$$

and, in an explicit form,

$$r_s(M) = \int_{\Pi_o} s\left(M_o\right) s^*\left(M_o - M\right) dM_o;$$

which is the self-correlation function of the signal. We know that a self-correlation function has a maximum modulus at the origin, or

$$r_s(0) = \int_{\Pi_o} |S\left(M_o\right)|^2 \, dM_o.$$

To be sure, the translated signal $s(M - M_1)$ will give a translated signal $r_s(M - M_1)$ having the same maximum but situated at the point $M = M_1$ instead of at the origin.

Likewise, response $r_b = s(M) \bigstar h(M)$ due to the noise becomes (keeping in mind IV.7) $r_b = b(M) \bigstar s^*(-M)$ or, in the explicit form,

$$r_b = \int_{\Pi_o} b\, M_o \; s^*\left(M_o - M\right) dM_o.$$

What conclusions can we draw from these expressions?

a) In the case of a white noise condition (IV.5) is satisfied and the signal/noise ratio (IV.3) becomes [23]

$$\rho = \frac{\text{energy in the signal}}{\text{spectral (energy) density of noise}}$$

In actual practice it can be said that condition (IV.5) is assured when the signal is only slightly correlated with the noise. Figure 43 gives an example of the extraction of words (signal) which are only slightly correlated to the noise (text).

b) If the noise is not white, which is often the case in practical problems, no conclusion can be drawn at all. It will be seen (Paragraph IV.5) that the response due to the noise may then be more perceptible than that due to signal. This will be prevented in the differentiation method.

4. The Experimental Arrangement

The device used both for the differentiation method and for the self-correlation method consists a) of a holographic assembly based on [23], which furnishes Fourier filters, and b) a restitutor which identifies the signals with the aid of the preceding filters.

a. The Fourier Holographic Filters

Let us take a model $s\left(M_o\right)$ of the signal whose presence in object $f\left(M_o\right)$ is to be detected. We have

$$s\left(M_o\right) \xrightarrow{F.T.} S(\Omega).$$

To make the identification we need (expression IV,6) a filter whose transparency is the complex function $t = S^*(\Omega)$. Except for certain very simple cases, it is impossible to realize such a function by currently available means (absorbent and dephasing deposits). By contrast, the holographic technique lends itself well to this operation [23].

To this end an assembly is constructed (Figure 39) which gives hologram filters with very low aberrations.

A spectrum analyzer, identical to that of the restitutor of Figure 34, gives in plane $\mathcal{F}$ the Fourier spectrum of a signal model $s\left(M_o\right)$ situated in plane Π_o. A part of the laser beam serves for forming a reference wave (shown cross-hatched) which is superimposed on the spectrum. The following reasoning is valid for any position of the reference source M_p, but it will be assumed, to simplify the proofs, that point M_p is situated in the object plane Π_o.

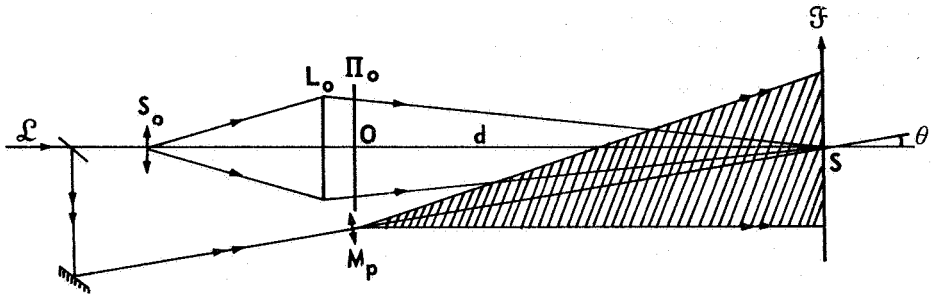

Figure 39. Hologram Filters: Recording Assembly. A spectrum analyzer, identical to that of the restitutor of Figure 35, gives in plane $\mathcal{F}$ the Fourier spectrum of the signal situated in object plane Π_o. Part of the laser beam $\mathcal{L}$ serves for forming a reference beam (crosshatched) originating from point M_p situated in plane Π_o. The photographic recording of the phenomenon in plane $\mathcal{F}$ is a Fourier hologram.

1) The signal diffracts on the spectral plane not the Fourier transform $S(\Omega)$ of $s(M_o)$ but (Appendix IV.1)

$$A_o(\Omega) = S(\Omega) \exp\left(i\varphi_o\right), \tag{IV.11}$$

the phase term $\exp(i\varphi_o)$ is independent of the nature of the signal; it is automatically compensated in a restitutor operating by double diffraction. However, in the present case where we use solely the spectrum analyzer part of the restitutor, this term persists and must be retained in the formulas.

2) The carrier wave originating from point $\acute{M}_p$ gives on plane $\mathcal{F}$ the following amplitude, standardized to module 1:

$$A_p(\Omega) = \exp\left(i\varphi_p\right). \tag{IV.12}$$

The phase $\varphi_p(\Omega)$ characterizes the spherical reference wave, i.e., the position of point M_p.

3) The photographic plate in $\mathcal{F}$ records the total illumination due to (IV.11) and (IV.12). The hologram obtained in this manner presents, according to expression (II.10), the transparency

$$t = 1 - \frac{\gamma}{2} A_p^* A_o - \frac{\gamma}{2} A_p A_o^* \tag{IV.13}$$

which becomes the following expression, keeping in mind (IV.11) and (IV.12) with the variable Ω instead of P used in Chapter II, and neglecting the constant $-\gamma/2$ which is of no importance,

$$(IV.14) \qquad t = 1 + S(\Omega)\ \exp\left[i\left(\varphi_o - \varphi_p\right)\right] + S^*(\Omega)\ \exp\left[-i\left(\varphi_o - \varphi_p\right)\right].$$

Let us make φ_o and φ_p explicit by taking S as the origin of the phases (Figure 39).

According to Appendix 1, φ_o represents the phase on $\mathcal{F}$ of a spherical wave of radius d having its center at 0, or

$$(IV.15) \qquad \varphi_o = \pi \lambda\, d\, \Omega^2.$$

Likewise, but by definition, φ_p represents the phase on $\mathcal{F}$ of a spherical wave originating from point M which -- let us recall -- is situated in plane Π_o. Whence, by a simple calculation,

$$(IV.16) \qquad \varphi_p = \pi \lambda\, d\, \Omega^2 - 2\pi\, \Omega.M_p\ .$$

As a result (IV.14) becomes

$$(IV.17) \qquad t = 1 + S(\Omega)\ \exp\left(2\pi i\, \Omega.M_p\right) + S^*(\Omega)\ \exp\left(-2\pi i\, \Omega.M_p\right).$$

Note that, independently of the use as a filter, this hologram makes it possible to reconstitute the recorded object or in this case the signal model to be identified.

Figure 40 shows such a restitution for the signal consisting of the word "filtrage." The two images -- direct and conjugate -- are both virtual because of the arrangement of Figure 39. Such a hologram is called a Fourier hologram, because the recording is carried out in the Fourier plane. Hence it is necessary to use the whole surface of the hologram in order to reconstitute the object correctly, contrary to the holograms in diffuse light. In effect, with only one portion $\Delta\Omega$, only the corresponding frequency band of the object can be reconstituted.

b. Restitution (Identification of the Signal)

In the restitutor (Figure 41) the object (= signal + noise)

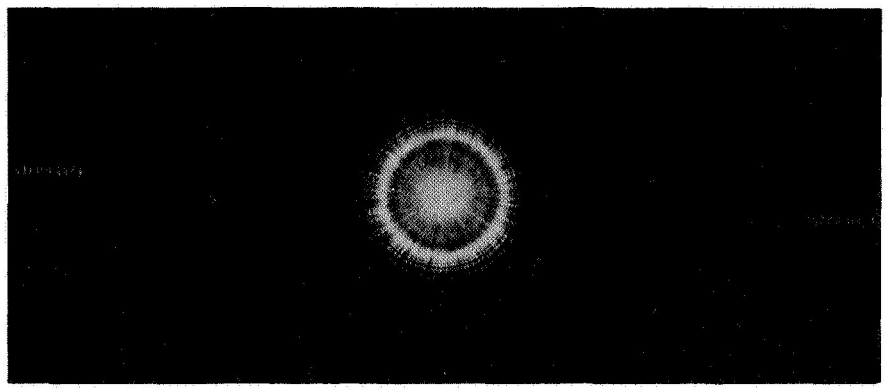

Figure 40. Percussional response of the filter used for the recognition of the word 'filtrage' in Figure 43.

(IV.18) $$f\left(M_o\right) = \varepsilon\left(M_o\right) + b\left(M_o\right),$$

is introduced in object plane Π_o.

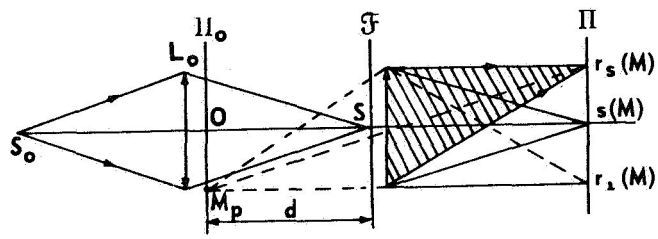

Figure 41. Pattern Recognition by Self-Correlation. The signal to be identified (in the presence of noise) is introduced in object plane Π_o of the restitutor. The Fourier hologram filter is arranged in the spectral plane $\mathcal{F}$. In the image plane we obtain, as in the case of an ordinary hologram, three spatially separated terms: $r_s(M)$ = self-correlation + noise; $s(M)$ = signal + noise; $r_1(M)$ = self-convolution + noise. The useful term is the self-correlation function of the signal.

Filter (IV.17) is introduced into the Fourier plane $\mathcal{F}$.

In that case three responses are obtained in the image plane Π, corresponding to the three terms of (IV.17), and in particular the response

sought, i.e., the sum of the self-correlation function of the signal $r_s(M)$ $s(M) \bigstar s^*(-M)$ and the noise-signal correlation function $r_b(M)$ $b(M) \bigstar s^*(-M)$.

To prove this, it is sufficient to follow the filtering scheme (expression IV.2) or, by doing our reasoning on the signal, for example,

(IV.19) $$s(M) \xrightarrow{F.T.} S(\Omega) \longrightarrow \otimes \longrightarrow S(\Omega)\ H(\Omega) \xrightarrow{F.T.^{-1}} r(M).$$
$$\Big| H(\Omega)$$

Function $H(\Omega)$ is the expression (IV.17) and, since the system is linear, it is sufficient to consider the three terms of (IV.17) separately.

(1) The Self-Correlation. The third term of (IV.17) is

$$H_3(\Omega) = S^*(\Omega)\ \exp\left(-2\pi i\, \Omega.M_p\right);$$

but

$$S(\Omega)\ S^*(\Omega) \xrightarrow{F.T.^{-1}} s(M) \bigstar s^*(-M) = r_s(M)$$

and

(IV.20) $$S\ S^*\ \exp\ 2\pi i\, \Omega.M_p \xrightarrow{F.T.^{-1}} r_s\left(M - M_p\right).$$

Thus the contribution of the third term of (IV.17) is the self-correlation function sought but, instead of having for center the origin of plane II, it has its center at point

(IV.21) $$M = M_p,$$

i.e., on the image which would be produced by the reference source on plane II if this source were present.

On Figure 41 the magnification is not standardized at $\gamma = +1$ as in the formulas, but where $\gamma = -1$, $r_s(M)$ has its center in $M = -M_p$.

(2) The Self-Convolution. The second term of (IV.17) is

(IV.22) $$H_2(\Omega) = S^*(\Omega)\ \exp\left(2\pi i\, \Omega.M_p\right).$$

Let us now set

(IV.23) $$r_1(M) = s(M) \bigstar s(M).$$

In plane II we obtain

(IV.24) $$S^2(\Omega)\ \exp\left(2\ \pi\ i\ \Omega.M_p\right) \xrightarrow{F.T.^{-1}} r_1\left(M + M_p\right);$$

$r_1\left(M + M_p\right)$ is the self-convolution function of $s(M)$, with its center in

(IV.25) $$M = - M_p$$

which is symmetrical to the center of the self-correlation function.

The term "having its center" is actually inaccurate because, while a self-correlation function exhibits a maximum at the origin $\left(\text{here } M_p\right)$ and possesses the symmetry property

(IV.26) $$|r_s\left(M - M_p\right)| = |r_s\left(M_p - M\right)|,$$

this is not so for the self-convolution function which possesses these two properties only for a symmetrical $s(M)$.

(3) The Central Term. The first term of (IV.17) gives

(IV.27) $$S(\Omega) \xrightarrow{F.T.^{-1}} s(M).$$

The signal is re-encountered in the center of plane II. In reality, in expression (IV.13) of the transparency of the hologram we have neglected (Paragraph II.2) certain terms, the result of which being that we obtain a slightly perturbed signal.

The three responses are separated in plane II, provided that we take a sufficiently large inclination of the carrier. In actual practice this occurs for (Figure 39)

(IV.28) $$OM_p > 2\ l,$$

where l is the half-object field.

In the same fashion, the noise in the object (IV.18) will give the three terms

(IV.29) $b(M)$ in the center,

(IV.30) $b(M) \bigstar s^*\left(M - M_p\right)$ around M_p,

(IV.31) $b(M) \bigstar s\left(M + M_p\right)$ around $- M_p$.

c. The Experimental Results

Figure 42 shows the assembly of the filters and of the restitution device.

Figure 43 gives an example of the recognition of words in a text; the responses are the maxima of the corresponding self-correlation functions. Figure 44 shows the "noise" due to successive superimpositions of the response (recognition of the word "filtrage").

It can be seen that for these examples the self-correlation method works well, because the words to be recognized are little correlated with the rest of the text, but it is quite obvious that if the noise-signal correlation is great, there will be ambiguity. This is notably the case with the recognition of isolated letters in a text; for example the identification of the letter I by self-correlation will also give undesirable responses for the letters which contain the I, i.e., B, D, E, F, H, K, L, M, P, R, T.

This circumstance is analyzed in Paragraph IV.5, and the solution which avoids the ambiguity is discussed in Paragraph IV.6.

d. Notes

(1) Realization of the Fourier Filters. If during the recording of the filter the reference source M_p is situated in the object plane Π_o (Figure 39), the three responses of Paragraph IV.4.b will form, on reconstruction, in the same plane Π. However M_p may be assigned any given position outside plane Π_o, hence holographic lenses are recorded as a result of which the three responses are formed in different planes.

(2) The Aberrations of the Filters. If the optical system presents aberrations, the signal/noise ratio may be considerably reduced. The same applies if the Fourier filters are aberrant.

To study the influence of the filters in this sense we must consider the assembly consisting of filter and restitutor.

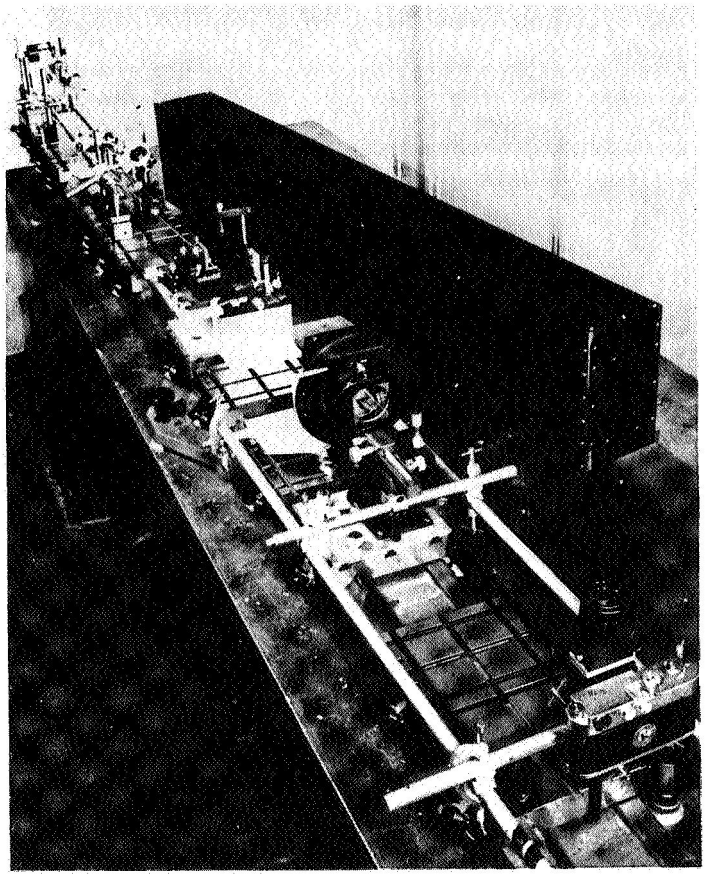

Figure 42. The restitutor and the assembly of Fourier filters.

(a)

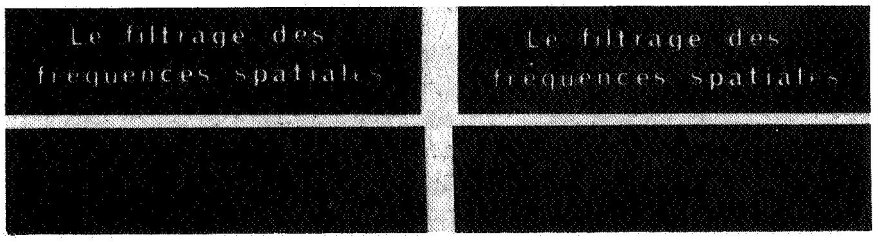

(b)

Figure 43. Identification of a word in a text by self-correlation: a) identification of the word 'des,' b) identification of the word 'filtrage.

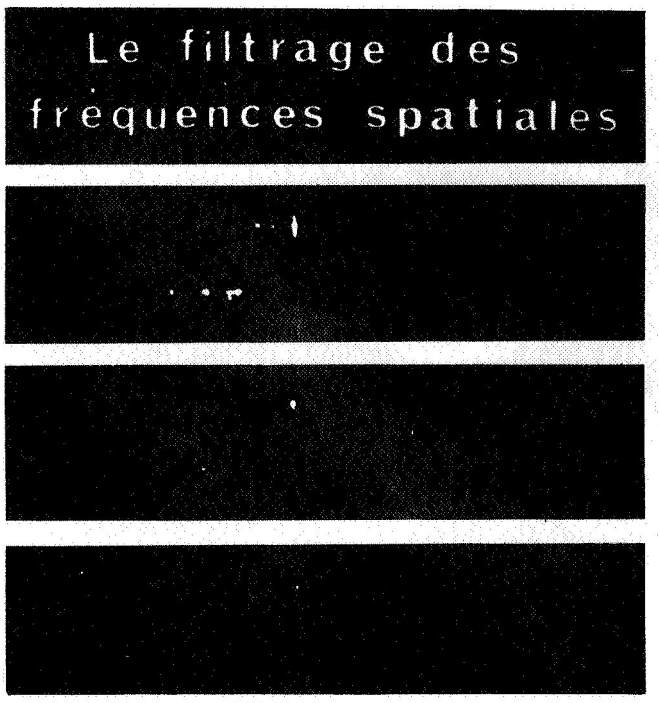

Figure 44. Aspect of Noise. Successive superimpositions (from bottom to top of the figure) of the response in the identification of the word 'filtrage.' During the measurements, results of the type shown in Figures 55 and 56 are obtained.

In the study carried out so far, all the phase terms have been developed to within the second order, which amounts to resorting to the paraxial approximation.

Now, it may be shown that, without carrying out any approximations and for any given position of the reference source M_p, we obtain the useful response (IV.20) with highly reduced aberrations, within the limits of validity of the Fourier formalism in optics.

To this end it is necessary that this formalism be effectively realized: this is the case of the device with convergent light which has been used (Appendix 2). Moreover it is necessary, for the correction of the holographic aberrations, that the spectrum analyzers of the restitutors and of the recording device of the filters be identical. In particular, the coma and the spherical aberration are then strictly zero.

(3) The Formalism in Pattern Recognition. In this case, it is sufficient, on the basis of the preceding results, to consider only the useful

response (IV.20) and the corresponding noise (IV.30), and to neglect the translation (due to the inclined reference wave) of the response in the image plane. The filtering scheme is then written as

$$\underset{\substack{\text{signal}\\ \text{noise}}}{s(M) + b(M)} \xrightarrow{\text{F. T.}} \underset{\text{spectrum}}{S(\Omega) + B(\Omega)} \xrightarrow{\otimes\ S^*(\Omega)\ \text{filter}} \xrightarrow{\text{F. T.}^{-1}} \begin{cases} r_s(M) = s(M) \bigstar s^*(-M) \\ + r_b(M) = b(M) \bigstar s^*(-M). \end{cases} \tag{IV.32}$$

5. Introduction to Identification by Differentiation

To show how one may identify a signal with a low probability of false alarm, it is necessary first of all to examine the reasons which bring about failures in the classical self-correlation method.

a. The Adapted Filter

Let us take an object $f(M) = s(M) + b(M)$ consisting of a signal $s(M)$ to be identified -- e.g., a printed letter -- in the presence of what, by extension, will be called noise $b(M)$, i.e., all the elements of the object other than $s(M)$ (the rest of the text).

When we identify the signal by means of a filter of transparency $S^*(\Omega)$, as in (IV.32), we obtain in the image plane II a self-correlation function r_s whose maximum ought to indicate a) the presence of the signal, b) the position of the signal (Cartesian coordinates of the maximum).

However, we obtain also the functions of the signal/noise intercorrelation r_b, and the latter may be much more perceptible than r_s. Thus a number of false responses are obtained in this manner.

In effect, in Paragraph IV.3 we have started out from the adapted filter

$$H(\Omega) = S^*(\Omega) / |B(\Omega)|^2. \tag{IV.33}$$

This filter gives good results in radar technique because the noise, which originates essentially from the reception chain, is known and it can often be considered as white in the reception band.

By contrast, in pattern recognition and, in particular, in the case of a printed text, the conditions are quite different. While the numerator of (IV.33) may be realized by holography (Paragraph IV.4.a), the denominator $1/|B(\Omega)|^2$ cannot generally be realized. In effect,

1) The noise b(M) is unknown, because we consider as noise all the unwanted letters of the text, and this is unknown;

2) The noise actually consists of undesirable signals of the same type as the signal to be identified; they have a limited support and their spectrum $B(\Omega)$ presents numerous zeros. Assuming the noise to be known, function $1/|B|^2$ can be realized only in a very approximate manner, by replacing an infinite transparency by a unit transparency;

3) even if we assume the noise to be known, it would be necessary to construct an antinoise filter for each page of the text.

Under these conditions we are led to the approximation

$$|B(\Omega)|^2 = \text{constant} \tag{IV.34}$$

Filter (IV.33) becomes $H(\Omega) = S^*(\Omega)$, and the response becomes, according to (IV.32):

$$r(M) = r_s(M) + r_b(M), \tag{IV.35}$$

whose first term

$$r_s(M) = s(M) \bigstar s^*(-M), \tag{IV.36}$$

due to the signal is the self-correlation function of the signal, and the second term

$$r_b(M) = b(M) \bigstar s^*(-M) \tag{IV.37}$$

is the signal/noise correlation function.

b. The Causes of Failure.

When the noise is highly correlated with the signal, the identification may become difficult and at times even impossible.

In effect, expression (IV.37) may be more readily perceptible than the self-correlation function (IV.36).

This is particularly striking in the extreme case where the noise contains the signal (example: the letter E contains the letter I). For simplification we shall assume that the signal and the noise have an amplitude of 1 in the regions s(M) and b(M) of respective areas Σ_s and Σ_b, with $\Sigma_s < \Sigma_b$. Furthermore, let us take c(M) as a region common to s(M) and b(M).

To sum up, then,

(IV.38) $$s(M) \subset b(m), \quad c(M) = s(M) \cap b(M).$$

From this it can be inferred that r_s and r_b have the same maximum, which is precisely

(IV.39) $$\int_{\Pi_o} |s(M)|^2 \, dM.$$

However, while $r_b(M)$ is maximum in a region having an area

(IV.40) $$\Sigma = \Sigma_b - \Sigma_s,$$

the self-correlation function $r_s(M)$ is maximum only at point M = 0. This means that while we look for s(M) we identify b(M).

c. Example

Let us illustrate this by an example. Take a text consisting of the two letters I and E (Figure 45a).

To simplify this demonstration we shall carry out our reasoning in one dimension — x — only.

Let the object be

(IV.41) $$f(x) = s(x) + b(x)$$

the signal to be identified is

(IV.42) $$I = s(x)$$

and the noise

(IV.43) $$E = b(x).$$

The distribution of the amplitudes in the object may be represented, along x, by two gates of different widths (Figure 45b).

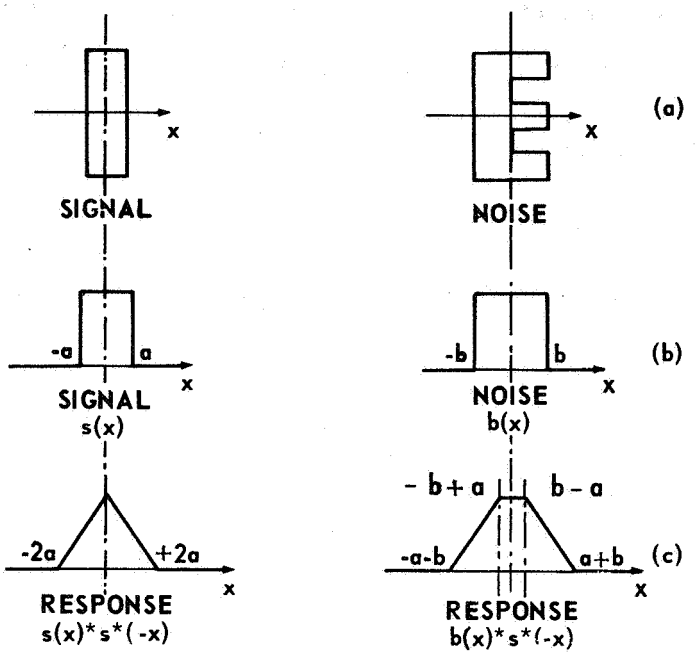

Figure 45. Disadvantages of the Method of Pattern Recognition by Self-Correlation. The object (a) gives the distribution of amplitudes (b) along x. If the object of line (b) is correlated with s(x), the response (c) consists of two terms: 1) a triangle which is a self-correlation function of the signal, and 2) a trapeze, which is a function of the signal/noise correlation.

The second term, which is much more perceptible than the first, has the result that it is the letter E that is identified while the letter I is sought. Compare this result with that of Figure 46.

The response (Figure 45c) consists of a triangle, a self-correlation function of the signal, and a trapeze, which is the signal/noise correlation function.

We note that the trapeze is much more readily perceptible than the triangle which, in principle, ought to permit the identification of the signal.

6. The Differentiation Method

a. Principle

Expression (IV. 40) shows that the ambiguity in the recognition is due to the finite surface of the elements considered. Now, a shape is generally defined by its contour and, more particularly, by its lines of discontinuity. The zones of constant or slowly varying amplitude play a minor role if it is desired to only recognize the presence and position of an object; thus they may be considered as a "noise" which one may get rid of, notably by differentiation.

Hence a suitable differential operator is applied to the object and the differentiated object is correlated with the signal to which the same operator has been applied. The differentiation is obtained simply by placing in the spectral plane $\mathfrak{F}$ an absorption filter having an appropriate law of transparency.

This will be made more explicit below in the one-dimensional and in the two-dimensional case.

For the following discussion let us remember that the experimental device used is the same as in Paragraph IV. 4, and that the filtering scheme adhered to is still (IV. 2).

b. The One-Dimensional Case

The principle of the method will seem more obvious if we went back to the example of Paragraph IV. 5. c relating to the case of simple self-correlation.

The object (Figure 46a) is differentiated (Figure 46b).

$$f'(x) = s'(x) + b'(x), \tag{IV. 41}$$

then it is correlated with the differentiated function $s'^{*}(x)$, which gives the response

$$r(x) = r_s(x) + r_b(x) \tag{IV. 42}$$

consisting of the response due to the signal sought

$$r_s(x) = s'(x) \bigstar s'^{*}(-x) \tag{IV. 43}$$

and of the response due to the noise

$$r_b(x) = b'(x) \bigstar s'^{*}(-x). \tag{IV. 44}$$

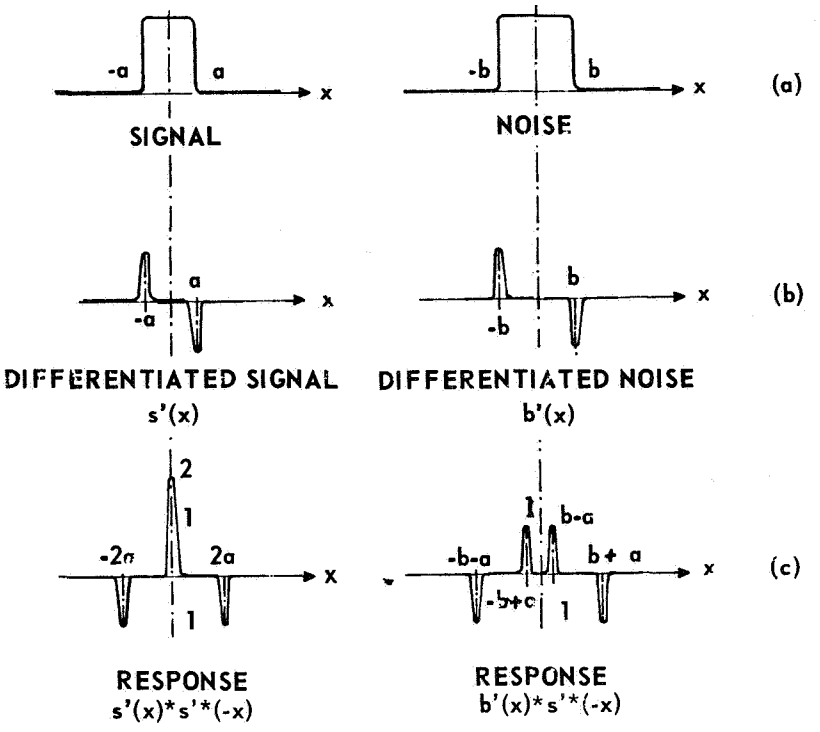

Figure 46. Pattern Recognition by Differentiation. The object (a) shown in the figure is the same as that of Figure 45. The differentiated object is shown in (b). If this object is correlated with a signal model which itself is differentiated, we obtain (c) where the useful response exhibits, with respect to the noise, a signal/noise ratio of 2 in amplitude and 4 in intensity.

The real signals are generally two-dimensional, in which case the signal/noise ratio is 16 for a similar example (Figure 47).

We then see on Figure 46c that the amplitude of the maximum of r_s is double its secondary maxima, and likewise the double of all the maxima due to the noise.

Hence the signal/noise ratio is 4 in intensity.

The objects generally considered are two-dimensional objects. For a similar example in x, y, the signal/noise ratio is then 16, instead of 1 as in the self-correlation example of Paragraph IV.5.c.

c. Form of the Fourier Filter

To determine the nature of the filter which leads to the results of the preceding paragraph, we must consider the Fourier plane. Let u be the

reduced variable in this plane. We then have, starting from the desired response,

$$s'(x) \bigstar s'^{*}(-x) \xrightarrow{F.T.} -4\pi^2 u^2 S(u)\, S^{*}(u), \tag{IV.45}$$

$$b'(x) \bigstar s'^{*}(-x) \xrightarrow{F.T.} -4\pi^2 u^2 B(u)\, S^{*}(u); \tag{IV.46}$$

hence the filtering scheme (IV.2) becomes (except for the coefficient $-4\pi^2$)

$$f(x) \xrightarrow{F.T.} F(u) \longrightarrow \otimes \xrightarrow{F.T.^{-1}} r(x) = f'(x) \bigstar s'^{*}(-x) \tag{IV.47}$$

$$\Big| \; u^2 S^{*}(u)$$

which shows that the filter consists of the product of u^2 and $S^{*}(u)$; i.e., brought about materially through juxtaposition

a) of a filter of transparency $S^{*}(u)$, which may be realized by holography (Paragraph IV.4.a), and

b) a filter whose law of transparency in amplitude is

$$t = u^2, \tag{IV.48}$$

or a parabolic transparency having a minimum 0 in the center.

This is possible, because the spectral plane $\mathcal{F}$ is limited by the entry diaphragm of lens L. If u_m is the radius of this diaphragm, the filter has the transparency in amplitude

$$\begin{cases} (u/u_m)^2 & \text{in the diaphragm,} \\ 0 & \text{outside the diaphragm.} \end{cases} \tag{IV.49}$$

d. The Two-Dimensional Case

To transpose the preceding reasoning to the two-dimensional case, it is necessary to differentiate the object f(M) and the percussional response $s^{*}(-M)$ of filter $S^{*}(\Omega)$ with respect to x and y. Then any differentiation will give a result. However, it is clear that the optimum operation is that which makes the "lines of the greatest slope" appear in the luminous distributions f(M) and $s^{*}(-M)$. This is obtained by the gradient operator

$$f(M) \Rightarrow \overrightarrow{\text{grad}}\, f(M), \qquad s^{*}(-M) \Rightarrow \overrightarrow{\text{grad}}\, s^{*}(-M). \tag{IV.50}$$

This gradient apparently has no physical meaning if considered in isolation. However, this is not so if we consider the whole recognition process in its entirety.

It is then shown (Appendix 3) that, if the diaphragm of lens L of the restitutor has a radius Ω_m, the two-dimensional filter has the form (also Paragraph IV. 6. c)

(IV. 51) $$H(\Omega) = (\Omega/\Omega_m)^2 S^*(\Omega) \text{ in the diaphragm}$$
$$H(\Omega) = 0 \text{ outside the diaphragm;}$$

the response due to the signal then becomes

(IV. 52) $$r_s = \int_{\Pi_o} \overrightarrow{\text{grad}}\, s(M_o) \cdot \overrightarrow{\text{grad}}\, s^*(M_o - M)\, dM_o$$

and the noise gives

(IV. 53) $$r_b = \int_{\Pi_o} \overrightarrow{\text{grad}}\, b(M_o) \cdot \overrightarrow{\text{grad}}\, s^*(M_o - M)\, dM_o.$$

These expressions are independent of the coordinate axes, and the detection of the lines of discontinuity depends neither on the form nor on the position of the objects, because the expression under the integration sign is a scalar product of gradients.

e. Differentiations of a Higher Order

In the same manner, if necessary by using a filter with $(\Omega/\Omega_m)^4$ we obtain for the signal (Δ representing the Laplacian operator)

(IV. 54) $$r_s = \Delta s(M) \bigstar \Delta s^*(-M)$$

and for the noise

(IV. 55) $$r_b = \Delta b(M) \bigstar \Delta s^*(-M)$$

The order of differentiations is limited only by the power of the lasers employed, because the differentiating filters have a maximum absorption at the center.

NOTE: An approximate differentiation, which consists in carrying out a high-pass filtering, gives satisfactory results in certain cases.

f. Experimental Results

Using the experimental device of Paragraph IV. 4 and the filters of form (IV. 51), the following results have been obtained:

Figure 47 is the two-dimensional illustration of the gate pulses of Paragraph IV. 6. b: a) the signal to be identified is indicated by an arrow; b) the response shows the presence and position of the signal without ambiguity. The signal/noise ratio is 26 dB (on the recording made with the aid of a film of $\gamma \simeq 2$).

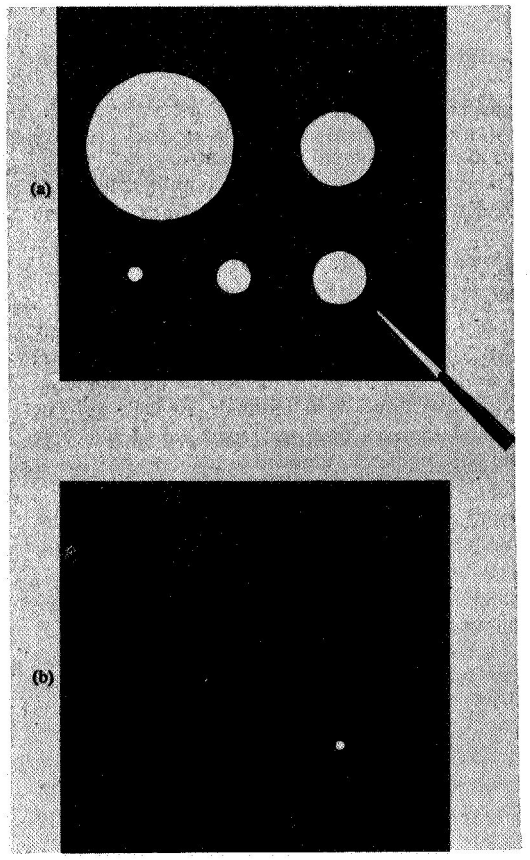

Figure 47. Method of Pattern Recognition by Differentiation. The signal to be identified in object (a) is indicated by an arrow. In the response (b) the signal/noise ratio is 26 dB.

Figure 48 shows two cases of fingerprint identification: (a) and (b) showing the signal, and (c) and (d) the corresponding responses.

Figure 49 relates to the identification of fingerprint (a) in the presence of print (b) having a very similar form; (c) is the response.

Figure 50 shows a fingerprint and its spectrum; we can see that it is difficult to realize such a Fourier spectrum by a method other than holography.

Figure 51 shows the identification of a letter in a text: in text (a) the signal to be identified is the letter "e"; the response is shown in (b), where all e's are simultaneously identified according to the properties of Paragraph IV. 2. b (automatic position-locating of the response).

Figure 52 shows an example analogous to that of Figure 51, but with different characters; in object (a) the signal is letter "e," while (b) is the response. We shall return to Figures 51 and 52 later on.

Figure 53 likewise shows the extraction of letter "s."

Finally, Figure 54 shows the extraction of letter O in the presence of two similar letters, C and Q; the response in (b) indicates a signal/noise ratio of 4 dB.

g. The Signal/Noise Ratio

This is greatly improved in the differentiation method, as we have seen. However this ratio always remains a function of the experimental conditions, and especially of the aberrations.

Figure 55 shows a microdensitogram of a line of the response (b) of Figure 51.

The text is plotted at the bottom of the figure, the letters being arranged opposite the corresponding peaks of the response; it is noted that the signal/noise ratio expressed in difference of density between the minimum "e" signal and the maximum noise is 0.12, or 1.2 dB.

The experimental device was equipped with good commercial lenses.

Figure 56 represents an analogous microdensitogram for the response of Figure 52; the signal/noise ratio has risen to 8 dB. The principal reason of the improvement is the use of a new optical system (calculated by the CERCO Company) which has been well corrected for aberrations; the latter are shown on Figure 57.

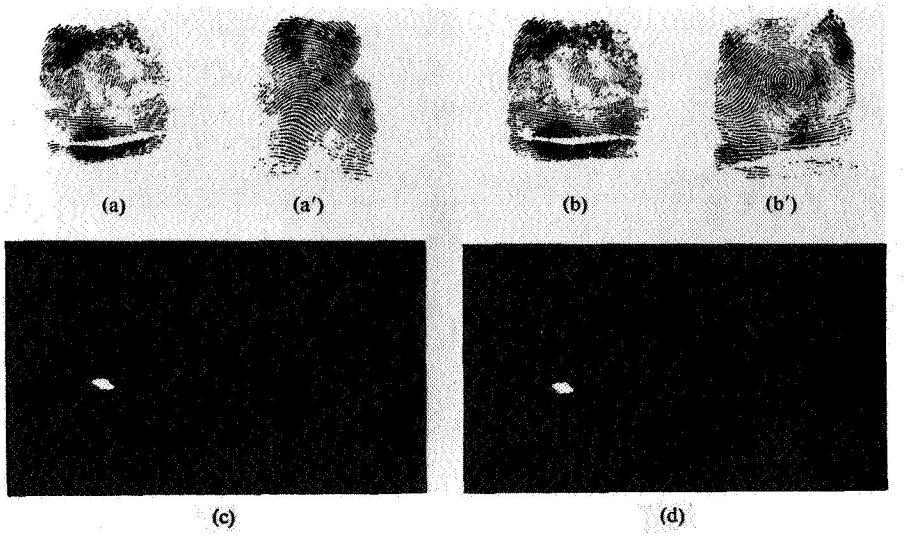

Figure 48. Differentiation Method. Identification of a fingerprint. Recognition of fingerprints (a) and (b) in the presence of fingerprints (a') and (b'). Responses (c) and (d) indicate the presence and position of fingerprints (a) and (b).

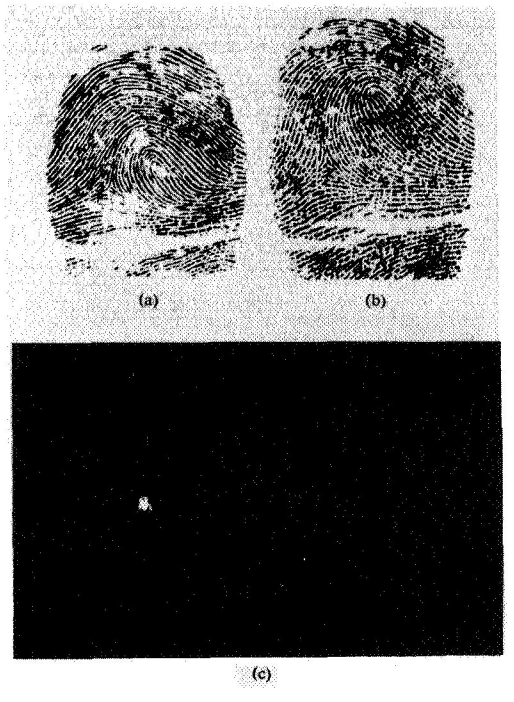

Figure 49. Differentiation Method. Identification of a fingerprint (a) in the presence of a very similar fingerprint (b). The response is shown in (c).

7. Conclusions on Pattern Recognition

Pattern recognition by differentiation consists merely in the juxtaposition, in the spectral plane of a restitutor operating by double diffraction, of

a) A filter whose transparency is proportional to the conjugate complex of the Fourier transform of the signal to be identified; this filter may be realized by holography;

b) An absorbent filter whose law of transmission entails the application of a differential operator to the object (signal + noise) and to the percussional response of the preceding filter.

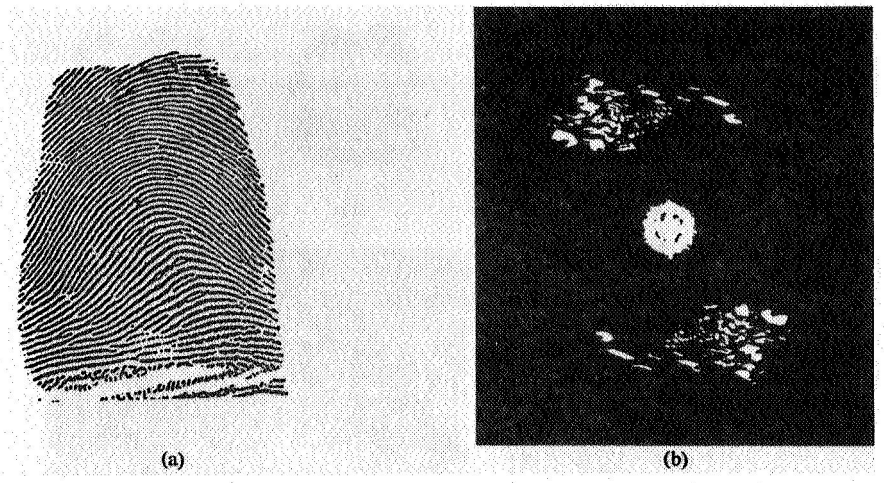

Figure 50. Example of an Object and of its Fourier Spectrum: a) object; b) spectrum.

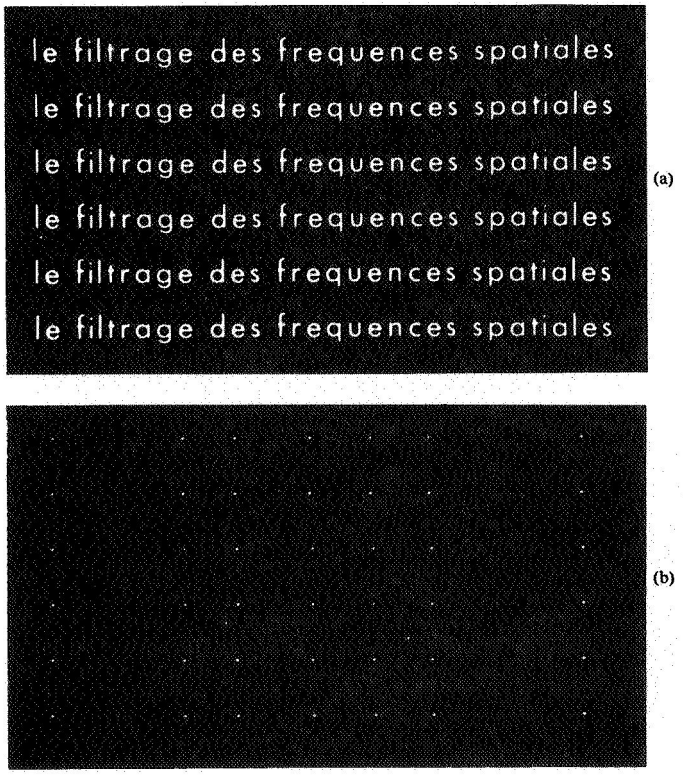

Figure 51. Method of Recognition by Differentiation. In object (a) the signal to be identified is the letter 'e.' The response (b) shows the simultaneous identification of all the 'e's' of the text (linearity of the optical system): the responses are formed automatically at the site of the corresponding letter.

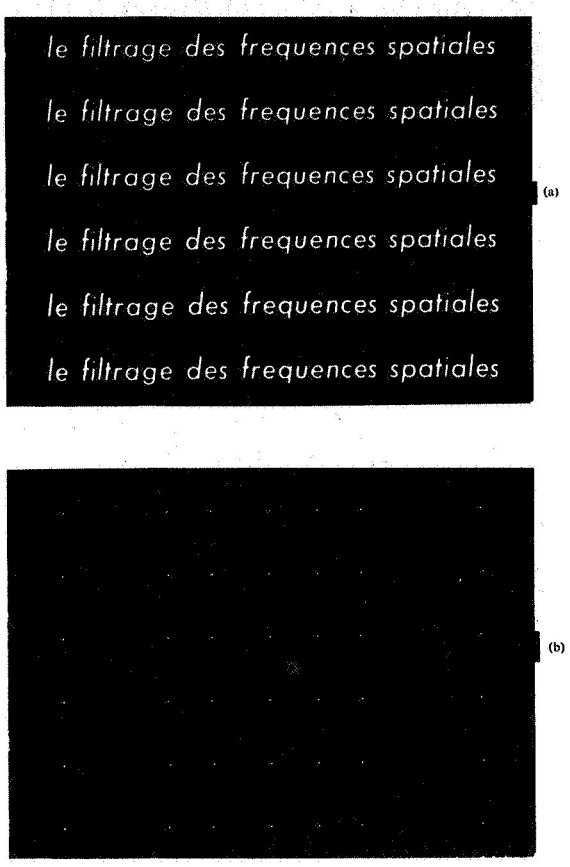

Figure 52. Method of Recognition by Differentiation. The signal to be identified in object (a) is the letter 'e.' Response shown in (b).

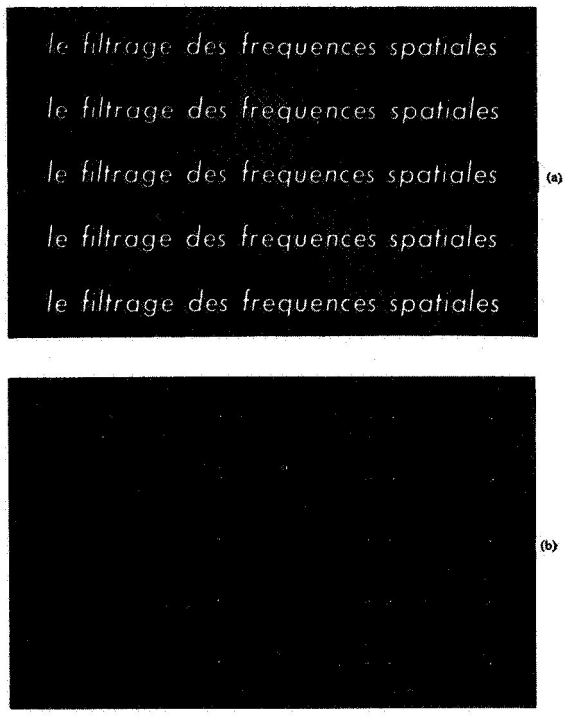

Figure 53. Method of Recognition by Differentiation. The signal to be identified is the letter 's' in text (a). Response is shown in (b).

If necessary, these two filters may be realized on a single support.

Efforts in this area have been directed essentially at the identification of characters in a printed text. The results obtained in this difficult case (the letters have very similar shapes and a character represents a small part of the total energy of the text) make it possible to envision the extension of the method to other types of signals, i.e., electrical or acoustic signals.

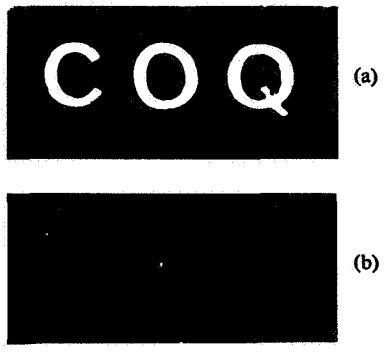

Figure 54. Differentiation Method. Identification of the the letter O among two other, very similar letters: a) text; b) response.

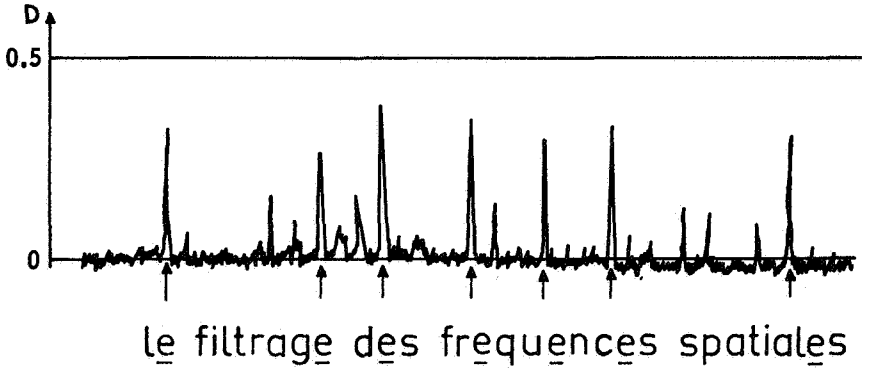

Figure 55. The Signal/Noise Ratio. On this microdensitogram of a line of the response of Figure 51, the text is plotted at the bottom of the figure, and the letters to be identified are underlined. The optical densities are plotted along the ordinate axis. The rather mediocre signal/noise ratio is due to the aberrations of the optical system and of the hologram filters.

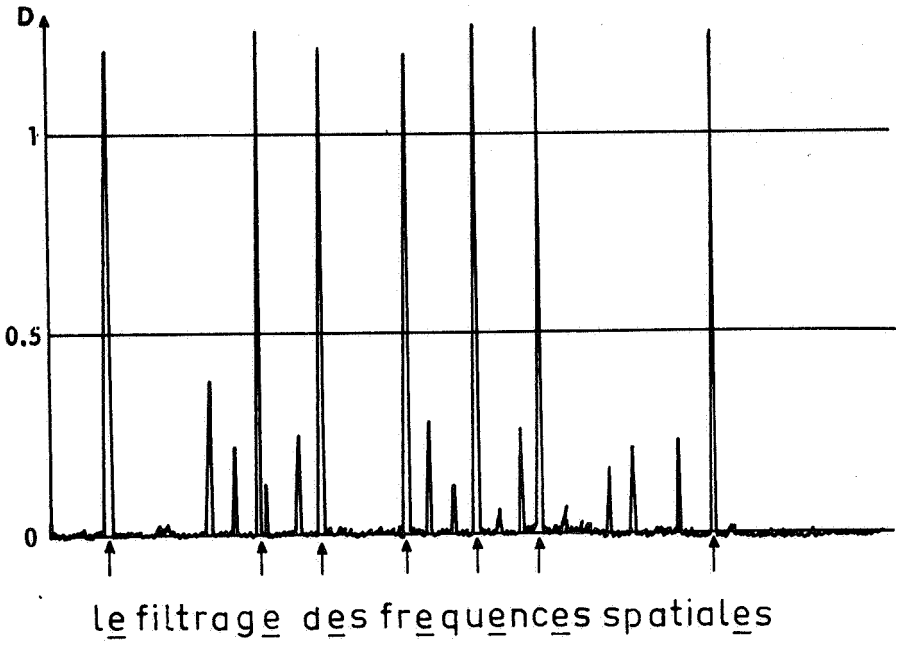

Figure 56. The Signal/Noise Ratio. This example, analogous to that of Figure 55, relates to the extraction of letter 'e' in Figure 52. The improvement of the signal/noise ratio is due to the correction of the aberrations of the optical system and of the hologram filters.

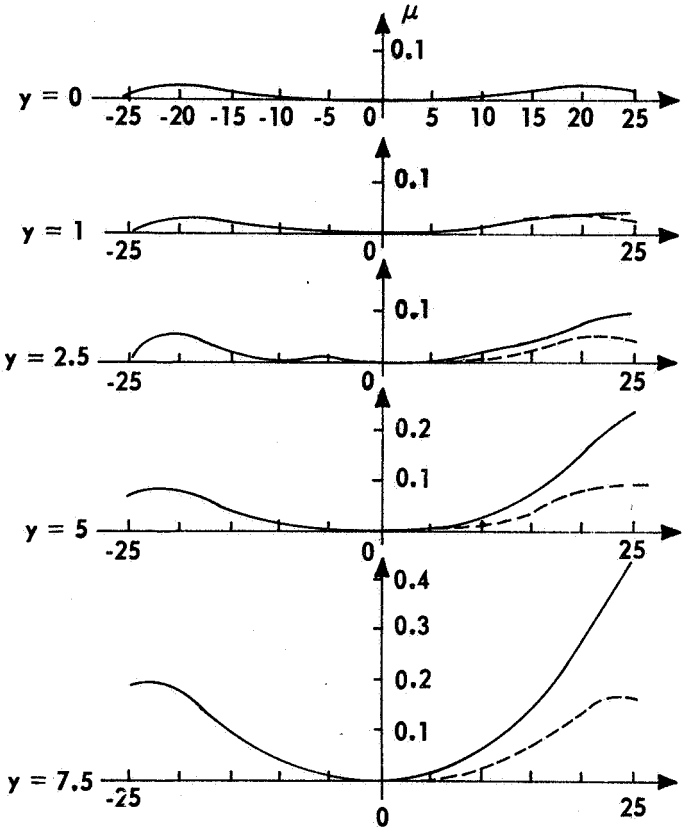

Figure 57. Lens L_o (or L) of the Restitutor. Wave surface for $\lambda = 6328$ Å. Tangential focal length (-) and sagittal focal length (----). Abscissa: aperture in millimeters; ordinate: deviations Δ in microns. Half-field denoted by y.

APPENDIX 1

Analysis of the Filtering of Spatial Frequencies

It is attempted to carry out optically the operation whose principle is schematically shown below:

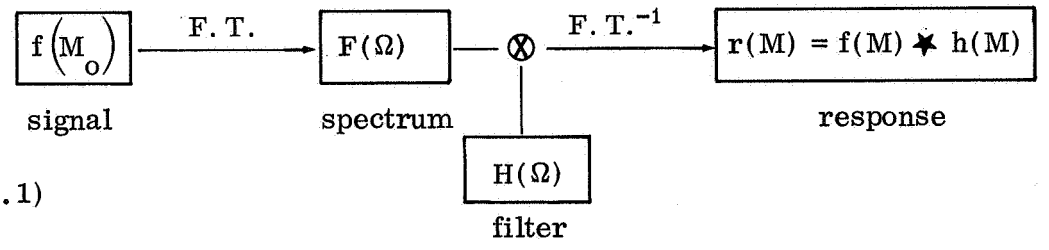

(A.1)

by means of the arrangement represented in Figure 58.

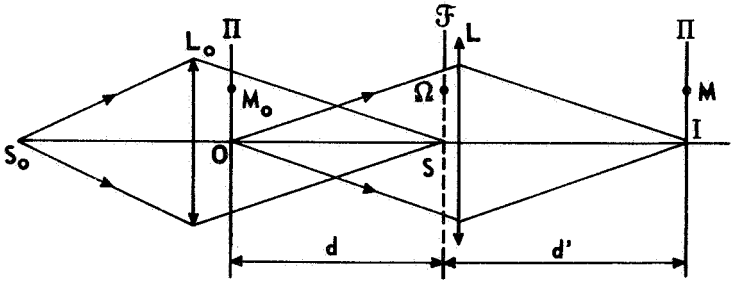

Figure 58.

It is shown [19] that to ensure linear filtering, the restitution lens L must have its entry diaphragm in the spectral plane $\mathcal{F}$. This is schematically represented by a simple lens placed in this plane.

1. Spectrum Analysis. Under the effect of the convergent coherent illumination originating from lens L_o, the signal $f(M_o)$ in plane Π_o diffracts, on plane $\mathcal{F}$ having a general point $P(x_1, y_1)$, the amplitude (expression I.16)

$$g(P) = \exp(i\, k\, P^2/2\, d)\; F(P), \tag{A.2}$$

where d is the distance between planes Π_o and $\mathcal{F}$, and F(P) the Fourier transform of $f(M_o)$. In reduced coordinates, with

$$\Omega = P/\lambda\, d, \tag{A.3}$$

expression (A.2) becomes, by writing $g(\Omega)$ and $F(\Omega)$ for $g(\lambda\, d\, \Omega)$ and $F(\lambda\, d\, \Omega)$,

$$g(\Omega) = \exp(i\, \pi\, \lambda\, d\, \Omega^2)\; F(\Omega)\,; \tag{A.4}$$

this spectrum is the product of the Fourier spectrum

$$F(\Omega) = \int_{\Pi_o} f\left(M_o\right) \exp\left(-\, 2\, \pi\, i\, \Omega . M_o\right) dM_o \tag{A.5}$$

and the quadratic phase factor

$$\exp(i\, \pi\, \lambda\, d\, \Omega^2)\,. \tag{A.6}$$

2. The Filtering. After passing through the filter of transparency $H(\Omega)$ placed in plane $\mathcal{F}$, wave (A.4) becomes

$$\exp(i\, \pi\, \lambda\, d\, \Omega^2)\; F(\Omega)\; H(\Omega)\,; \tag{A.7}$$

hence term (A.6) has no effect on the filtering. However it must be compensated in order that the restitution operation give a good inverse Fourier transform of the product $F(\Omega)\; H(\Omega)$.

3. The Restitution. It is known that a lens of focal length l introduces in its plane (plane $\mathcal{F}$) the phase difference

$$\exp(-\, i\, k\, P^2/2\, l)\,, \tag{A.8}$$

or, in reduced coordinates

$$\exp(-\, i\, \pi\, \lambda\, d^2\, \Omega^2/l)\,. \tag{A.9}$$

After passing through lens L, the wave (A.7) consequently becomes

$$g_1(\Omega) = \exp\left[\, i\, \pi\, \lambda\, d^2\, \Omega^2\, \left(\frac{1}{d} - \frac{1}{l}\right)\right] \; F(\Omega)\; H(\Omega)\,. \tag{A.10}$$

This wave gives, by diffraction on a plane at a distance d' from $\mathcal{F}$, an amplitude distribution $r(M)$, which is obtained by application of formula (I.7) relating to the Fresnel diffraction. This is written, in reduced coordinates, as

$$r(M) = \int_{\mathcal{F}} g_1(\Omega)\; \exp[i\, k(M - \lambda\, d\, \Omega)^2/2\, d']\; d\Omega \tag{A.11}$$

whence, by expanding the exponent and taking (A.10) into account,

$$(A.12)\quad r(M) = \exp\left(i\frac{\pi M^2}{\lambda d'}\right)\int_{\mathcal{F}} e^{i\varphi}\, F(\Omega)\, H(\Omega)\, \exp\left(-2\pi i \frac{d}{d'}\,\Omega.M\right) d\Omega,$$

with

$$(A.13)\qquad \varphi = \pi\lambda d^2\,\Omega^2\left(\frac{1}{d}+\frac{1}{d'}-\frac{1}{l}\right).$$

Now, since Π_o and Π are conjugate planes, we have

$$(A.14)\qquad \frac{1}{d}+\frac{1}{d'}-\frac{1}{l}=0;$$

hence

$$(A.15)\qquad e^{i\varphi}=1.$$

Moreover, (A.12) is the final result of the filtering; at this stage the recording is made by a quadratic detector and the phase term

$$(A.16)\qquad \exp(i\,\pi M^2/\lambda d')$$

disappears. It may therefore be neglected. Hence (A.12) becomes

$$(A.17)\qquad r(M) = \int_{\mathcal{F}} F(\Omega)\, H(\Omega)\, \exp\left(-2\pi i\frac{d}{d'}\,\Omega.M\right) d\Omega$$

which represents the inverse Fourier transform of the product

$$(A.18)\qquad R(\Omega) = F(\Omega)\, H(\Omega)$$

which, except for a scale term, is magnification $\lambda = -d'/d$ of lens L.

Standardizing γ at 1, we have, as a result,

$$(A.19)\qquad R(\Omega) \xrightarrow{F.T.^{-1}} r(M) = f(M) \bigstar h(M).$$

Therefore the filtering follows the schematic outline of (A.1), with the phase term (A.6) having been compensated and term (A.16) disappearing during the recording.

Nevertheless, in Fourier transform holography it is necessary to keep (A.6) in mind, and if response (A.12) must be taken up by another coherent system, it is also necessary to take (A.16) into account.

APPENDIX 2

Definitions Relating to the Photographic Emulsions

We define the following parameters for the photographic emulsions:

1. Transparency in Intensity. This is the ratio, T, of the emergent fluxes Φ_1 and the incident fluxes Φ_0 at each point of the emulsion on which the image is prepared:

(A.20) $$T = \Phi_1/\Phi_0, \quad 0 \leq T \leq 1.$$

Thus the transparency T varies with each point of coordinates x, y on the emulsion, and it defines a function T(x, y) of these coordinates.

2. Optical Density.

(A.21) $$D = \log(1/T).$$

3. Lumination. This is the energy W received by the plate, or the product of illumination E and the exposure time τ

(A.22) $$W = E\,\tau.$$

4. Characteristic (or Blackening) Curve. This curve gives the variations of density as a function of lumination (Figure 59). This curve often includes a straight-line portion whose slope γ is also called contrast factor. The straight-line portion has the form

(A.23) $$D = \gamma \log(W/W_0),$$

where W_0 is a constant.

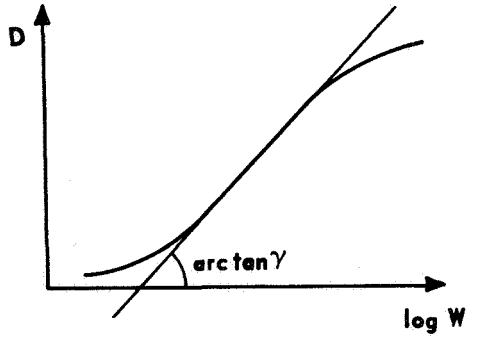

Figure 59.

According to (A.21) we then have $T = (W/W_0)^{-\gamma}$, or

(A.24) $$T = C\,E^{-\gamma};$$

E is the illumination received by the plate and C a constant which depends notably on the exposure time, on the sensitivity of the plate and on factor γ.

5. Transparency in Amplitude. In coherent optics it is the (complex) amplitudes of the waves which intervene; then the transparency in amplitude is defined as the ratio (t) of the emergent amplitude (A_1) and incident amplitude (A_0) at each point of the emulsion on which the image is produced.

(A.25) $$t = A_1/A_0, \quad 0 \leq |t| \leq 1.$$

$t(x,y)$ is a real or complex function of coordinates x, y on the emulsion; its modulus is less than 1.

We also have the relations

(A.26) $$T = t\, t^*$$

and, for a real t, $t = T^{\frac{1}{2}}$, or

(A.27) $$t = C' E^{-\gamma/2},$$

where C' is a constant.

APPENDIX 3

The Two- Dimensional Differentiating Filters

Let us take an identification by classical self-correlation

$$r(M) = f(M) \bigstar s^*(-M). \tag{A.28}$$

The detection of the lines of discontinuity (Paragraph IV.6.4) leads to the determination of the linear differential operators L which, when applied to the object

$$f(M) = s(M) + b(M) \tag{A.29}$$

and to the percussional response of the Fourier filter

$$s^*(-M) \tag{A.30}$$

give a result

(A.31)
- a) independent of the coordinate axes;
- b) independent of the shape of the signals treated, i.e., of their position and orientation.

Now let us express the Dirac distribution by $\delta(M) = \delta(x,y)$ (see, for example [17] for the mathematical formalism), and let the linear differential operator be

$$L(M) = L(x,y) = \sum \left(a_m \frac{\partial^m \delta}{\partial x^m} + b_n \frac{\partial^n \delta}{\partial y^n} + c_p \frac{\partial^p \delta}{\partial x^q \partial y^{p-q}} \right) \tag{A.32}$$

which, when applied to (A.29) and (A.30), transforms (A.28) into

$$\begin{aligned} r_1(M) &= [L \bigstar f(M)] \bigstar [L \bigstar s^*(-M)] \\ &= L \bigstar L \bigstar r(M). \end{aligned} \tag{A.33}$$

The Fourier transform in $\Omega(u,v)$ of $r(M)$ is

$$R(\Omega) = F(\Omega)\, S^*(\Omega), \tag{A.34}$$

The Fourier transform of L is

$$(A.35) \qquad \tilde{L} = \Sigma \left[a_m (2\pi i u)^m + b_n (2\pi i v)^n + c_p (2\pi i)^p u^q v^{p-q} \right]$$

and that of (A.33)

$$(A.36) \qquad R_1(\Omega) = \tilde{L}^2 R(\Omega) .$$

To satisfy (A.31) it is necessary that $\tilde{L}^2$ have a radial symmetry

$$\tilde{L}^2 = a(2\pi i)^{2n} (u^2 + v^2)^n = a(2\pi i \Omega)^{2n},$$

where n is a whole number and a a constant which will be subsequently neglected.

Then the response (A.33) becomes

$$(A.37) \qquad r_1(M) = r(M) \bigstar F.T.^{-1} \{-4\pi^2(u^2 + v^2)\}^n .$$

Then it is necessary to distinguish between several cases, depending on the value of n.

1. Example of n = 1. We have

$$(A.38) \qquad -4\pi^2(u^2 + v^2) \xrightarrow{F.T^{-1}} \frac{\partial^2 \delta}{\partial x^2} + \frac{\partial^2 \delta}{\partial y^2} .$$

As a result the response (A.37) becomes (keeping A.28 in mind)

$$(A.39) \qquad r_1(M) = \left(\frac{\partial^2 \delta}{\partial x^2} + \frac{\partial^2 \delta}{\partial y^2} \right) \bigstar f(M) \bigstar s^*(-M) .$$

This convolution product is distributive relative to the addition and to the differentiation, whence

$$(A.40) \qquad r_1(M) = \frac{\partial f(M)}{\partial x} \bigstar \frac{\partial s^*(-M)}{\partial x} + \frac{\partial f}{\partial y} \bigstar \frac{\partial s^*(-M)}{\partial y} .$$

Now $\partial f/\partial x$, $\partial f/\partial y$ and $\partial s^*(-M)/\partial x$, $\partial s^*(-M)/\partial y$ are the components of $\overrightarrow{\text{grad}}\, f(M)$ and $\overrightarrow{\text{grad}}\, s^*(-M)$; hence (A.40) is written -- by making the convolution products explicit -- as the sum of a scalar product

(A.41) $$r_1(M) = \int_{\Pi_o} \overrightarrow{\text{grad}}\, f(M_o) \cdot \overrightarrow{\text{grad}}\, s^*(M_o - M)\, dM_o.$$

2. Example of n = 2. We have

$$16\,\pi^4(u^2 + v^2)^2 \xrightarrow{\text{F. T.}^{-1}} \Delta\delta \bigstar \Delta\delta.$$

Then the response (A.37) is written as

$$r_1(M) = \Delta\delta \bigstar f(M) \bigstar \Delta\delta \bigstar s^*(-M)$$

or also as

$$r_1(M) = \Delta f(M) \bigstar \Delta s^*(-M).$$

REFERENCES

1. A. Maréchal and P. Croce, Proceedings of the Academy of Sciences, 237, 1953, p. 667.

2. D. Gabor, Nature, 161, 1948, p. 777.

3. E. Leith and J. Upatnieks, J. Opt. Soc. Amer., 54, 1964, p.1295.

4. G. W. Stroke, Eng. Sum. Conf. Ann Arbor, Michigan, 1964.

5. P. Croce, Thesis, Rev. Opt., 35, 1956, pp. 569 and 642.

6. MM. Marquet, Opt. Acta, 6, 1959, p. 404.

7. J. Tsujiuchi, Opt. Acta, 7, 1960, p. 243.

8. A. Sommerfeld, Optics, Acad. Press, New York, 1954, p. 201.

9. R. W. Meier, J. Opt. Soc. Amer., 55, 1965, p. 987.

10. M. M. Marquet and H. Royer, "Study of the Geometric Aberrations of Images Reconstituted by Holography, DRME Pamphlet," 1965.

11. M. M. Marquet and H. Royer, Proceedings of the Academy of Sciences, 260, 1965, p. 6051.

12. S. Lowenthal and Y. Belvaux, Proceedings of the Academy of Sciences [B], 263, 1966, p. 904.

13. G. W. Stroke and A. Labeyrie, Appl. Phys. Letters, 6, 1966, p.42.

14. L. O. Heflinger, R. F. Wuerker and R. E. Brooks, J. Appl. Physics, 37, 1966, p. 642.

15. F. S. Harris, G. C. Sherman, and B. H. Billings, Appl. Optics, 5, 1966, p. 665.

16. E. L. O'Neill, Inst. Radio Engrs. Trans. Inf. Th., IT-2, 1956, p. 56.

17. J. Arsac, Fourier Transformation andTheory of Distributions, Dunod, Paris, 1961.

REFERENCES (Concluded)

18. A. Maréchal and M. Françon, "Diffraction, Structure of Images," Rev. Opt., Paris, 1960.

19. S. Lowenthal, Opt. Acta., 12, 1965, p. 261.

20. S. Lowenthal and Y. Belvaux, Proceedings of the Academy of Sciences [B], 262, 1966, p. 413.

21. S. Lowenthal and Y. Belvaux, Opt. Acta, 14, 1967, p. 245.

22. G. L. Turin, Inst. Radio Engrs. Trans. Inf. Th., IT-6, No. 3, 1960, p. 311.

23. A. van der Lugt, Inst. Elec. Engrs. Trans. Inf. Th., 4, 1964, p. 139.

DISTRIBUTION

EXTERNAL

	No. of Copies
Air University Library ATTN: AUL3T Maxwell Air Force Base, Alabama 36112	1
U. S. Army Electronics Proving Ground ATTN: Technical Library Fort Huachuca, Arizona 85613	1
Naval Weapons Center ATTN: Technical Library, Code 753 China Lake, California 93555	1
Naval Weapons Center, Corona Laboratories ATTN: Documents Librarian Corona, California 91720	1
Lawrence Radiation Laboratory ATTN: Technical Information Division P. O. Box 808 Livermore, California 94550	1
Sandia Corporation ATTN: Technical Library P. O. Box 969 Livermore, California 94551	1
U. S. Naval Postgraduate School ATTN: Library Monterey, California 93940	1
Electronic Warfare Laboratory, USAECOM Post Office Box 205 Mountain View, California 94042	1
Jet Propulsion Laboratory ATTN: Library (TDS) 4800 Oak Grove Drive Pasadena, California 91103	2
U. S. Naval Missile Center ATTN: Technical Library, Code N3022 Point Mugu, California 93041	1
U. S. Army Air Defense Command ATTN: ADSX Ent Air Force Base, Colorado 80912	1
Central Intelligence Agency ATTN: OCR/DD-Standard Distribution Washington, D. C. 20505	4
Harry Diamond Laboratories ATTN: Library Washington, D. C. 20438	1
Scientific & Tech. Information Div., NASA ATTN: ATS Washington, D. C. 20546	1
U. S. Atomic Energy Commission ATTN: Reports Library, Room G-017 Washington, D. C. 20545	1
U. S. Naval Research Laboratory ATTN: Code 2027 Washington, D. C. 20390	1
Weapons Systems Evaluation Group Washington, D. C. 20305	1
John F. Kennedy Space Center, NASA ATTN: KSC Library, Documents Section Kennedy Space Center, Florida 32899	2
APGC (PGBPS-12) Eglin Air Force Base, Florida 32542	1
U. S. Army CDC Infantry Agency Fort Benning, Georgia 31905	1
Argonne National Laboratory ATTN: Report Section 9700 South Cass Avenue Argonne, Illinois 60440	1
U. S. Army Weapons Command ATTN: AMSWE-RDR Rock Island, Illinois 61201	1
Rock Island Arsenal ATTN: SWERI-RDI Rock Island, Illinois 61201	1
U. S. Army Cmd. & General Staff College ATTN: Acquisitions, Library Division Fort Leavenworth, Kansas 66027	1
Combined Arms Group, USACDC ATTN: Op. Res., P and P Div. Fort Leavenworth, Kansas 66027	1
U. S. Army CDC Armor Agency Fort Knox, Kentucky 40121	1
Michoud Assembly Facility, NASA ATTN: Library, I-MICH-OSD P. O. Box 29300 New Orleans, Louisiana 70129	1
Aberdeen Proving Ground ATTN: Technical Library, Bldg. 313 Aberdeen Proving Ground, Maryland 21005	1
NASA Sci. & Tech. Information Facility ATTN: Acquisitions Branch (S-AK/DL) P. O. Box 33 College Park, Maryland 20740	5
U. S. Army Edgewood Arsenal ATTN: Librarian, Tech. Info. Div. Edgewood Arsenal, Maryland 21010	1

	No. of Copies
National Security Agency ATTN: C3/TDL Fort Meade, Maryland 20755	1
Goddard Space Flight Center, NASA ATTN: Library, Documents Section Greenbelt, Maryland 20771	1
U. S. Naval Propellant Plant ATTN: Technical Library Indian Head, Maryland 20640	1
U. S. Naval Ordnance Laboratory ATTN: Librarian, Eva Liberman Silver Spring, Maryland 20910	1
Air Force Cambridge Research Labs. L. G. Hanscom Field ATTN: CRMXLR/Stop 29 Bedford, Massachusetts 01730	1
U. S. Army Tank Automotive Center ATTN: SMOTA-RTS.1 Warren, Michigan 48090	1
U. S. Army Materials Research Agency ATTN: AMXMR-ATL Watertown, Massachusetts 02172	1
Strategic Air Command (OAI) Offutt Air Force Base, Nebraska 68113	1
Picatinny Arsenal, USAMUCOM ATTN: SMUPA-VA6 Dover, New Jersey 07801	1
U. S. Army Electronics Command ATTN: AMSEL-CB Fort Monmouth, New Jersey 07703	1
Sandia Corporation ATTN: Technical Library P. O. Box 5800 Albuquerque, New Mexico 87115	1
ORA(RRRT) Holloman Air Force Base, New Mexico 88330	1
Los Alamos Scientific Laboratory ATTN: Report Library P. O. Box 1663 Los Alamos, New Mexico 87544	1
White Sands Missile Range ATTN: Technical Library White Sands, New Mexico 88002	1
Rome Air Development Center (EMLAL-1) ATTN: Documents Library Griffiss Air Force Base, New York 13440	1
Brookhaven National Laboratory Technical Information Division ATTN: Classified Documents Group Upton, Long Island, New York 11973	1
Watervliet Arsenal ATTN: SWEWV-RD Watervliet, New York 12189	1
U. S. Army Research Office (ARO-D) ATTN: CRD-AA-IP Box CM, Duke Station Durham, North Carolina 27706	1
Lewis Research Center, NASA ATTN: Library 21000 Brookpark Road Cleveland, Ohio 44135	1
Foreign Technology Division ATTN: Library Wright-Patterson Air Force Base, Ohio 45400	1
U. S. Army Artillery & Missile School ATTN: Guided Missile Department Fort Sill, Oklahoma 73503	1
U. S. Army CDC Artillery Agency ATTN: Library Fort Sill, Oklahoma 73504	1
U. S. Army War College ATTN: Library Carlisle Barracks, Pennsylvania 17013	1
U. S. Naval Air Development Center ATTN: Technical Library Johnsville, Warminster, Pennsylvania 18974	1
Frankford Arsenal ATTN: C-2500-Library Philadelphia, Pennsylvania 19137	1
Div. of Technical Information Ext., USAEC P. O. Box 62 Oak Ridge, Tennessee 37830	1
Oak Ridge National Laboratory ATTN: Central Files P. O. Box X Oak Ridge, Tennessee 37830	1
Air Defense Agency, USACDC ATTN: Library Fort Bliss, Texas 79916	1
U. S. Army Air Defense School ATTN: AKBAAS-DR-R Fort Bliss, Texas 79906	1

	No. of Copies
U. S. Army Combat Developments Command Institute of Nuclear Studies Fort Bliss, Texas 79916	1
Manned Spacecraft Center, NASA ATTN: Technical Library, Code BM6 Houston, Texas 77058	1
Defense Documentation Center Cameron Station Alexandria, Virginia 22314	20
U. S. Army Research Office ATTN: STINFO Division 3045 Columbia Pike Arlington, Virginia 22204	1
U. S. Naval Weapons Laboratory ATTN: Technical Library Dahlgren, Virginia 22448	1
U. S. Army Engineer Res. & Dev. Labs. ATTN: Scientific & Technical Info. Br. Fort Belvoir, Virginia 22060	2
Langley Research Center, NASA ATTN: Library, MS-185 Hampton, Virginia 23365	1
Research Analysis Corporation ATTN: Library McLean, Virginia 22101	1
Foreign Science & Technology Center Munitions Building Washington, D. C. 20315	3
National Aeronautics & Space Administration Code USS-T (Translation Section) Washington, D. C. 20546	2

	No. of Copies
INTERNAL	
Headquarters U. S. Army Missile Command Redstone Arsenal, Alabama 35809	
ATTN: AMSMI-D	1
AMSMI-XE, Mr. Lowers	1
AMSMI-Y	1
AMSMI-R, Mr. McDaniel	1
AMSMI-RAP	1
AMSMI-RBLD	10
USACDC-LnO	1
AMSMI-RB, Mr. Croxton	1
AMSMI-RBT	8
National Aeronautics & Space Administration Marshall Space Flight Center Marshall Space Flight Center, Alabama 35812	
ATTN: MS-T, Mr. Wiggins	5
R-P&VE-PE, Mr. Bock	1

DOCUMENT CONTROL DATA - R & D

(Security classification of title, body of abstract and indexing annotation must be entered when the overall report is classified)

1. ORIGINATING ACTIVITY *(Corporate author)*
Redstone Scientific Information Center
Research and Development Directorate
U. S. Army Missile Command
Redstone Arsenal, Alabama 35809

2a. REPORT SECURITY CLASSIFICATION
Unclassified

2b. GROUP
N/A

3. REPORT TITLE
RECENT ADVANCES IN COHERENT OPTICS: FILTERING OF SPATIAL FREQUENCIES; HOLOGRAPHY
Revue d'Optique, Theorique et Instrumentale, 46, No. 1, pp. 1-64 (1967)

4. DESCRIPTIVE NOTES *(Type of report and inclusive dates)*
Translated from the French

5. AUTHOR(S) *(First name, middle initial, last name)*
Serge Lowenthal
Yves Belvaux

6. REPORT DATE
28 March 1968

7a. TOTAL NO. OF PAGES
100

7b. NO. OF REFS
15

8a. CONTRACT OR GRANT NO.
N/A

b. PROJECT NO.
N/A

c.

d.

9a. ORIGINATOR'S REPORT NUMBER(S)
RSIC - 769

9b. OTHER REPORT NO(S) *(Any other numbers that may be assigned this report)*
AD

10. DISTRIBUTION STATEMENT
This document has been approved for public release and sale; its distribution is unlimited.

11. SUPPLEMENTARY NOTES
None

12. SPONSORING MILITARY ACTIVITY
Redstone Scientific Information Center
Research and Development Directorate
U. S. Army Missile Command
Redstone Arsenal, Alabama 35809

13. ABSTRACT

New applications of coherent light are presented:

a) Holography: recording of three-dimensional objects; diffuse illumination interferometry; reproduction of holograms; Fourier - transform holography and geometrical properties of holograms;

b) Spatial filtering: optical data processing, especially pattern recognition; automatic reading of characters, identification of fingerprints and other signals.

DD FORM 1 NOV 68 1473 REPLACES DD FORM 1473, 1 JAN 64, WHICH IS OBSOLETE FOR ARMY USE.

14. KEY WORDS	LINK A		LINK B		LINK C	
	ROLE	WT	ROLE	WT	ROLE	WT
Coherent optics						
Diffraction						
Three-dimensional holograms						
Fourier - transform holography						
Spatial frequencies						
Optical images						
Data processing						
Pattern recognition						